

(19) World Intellectual Property Organization
International Bureau



(43) International Publication Date
22 October 2009 (22.10.2009)

(10) International Publication Number
WO 2009/129265 A1

(51) International Patent Classification:
A61B 5/05 (2006.01)

(74) Agents: AVAKIAN, Patrick et al.; Davis Wright Tremaine LLP, 865 South Figueroa Street, Suite 2400, Los Angeles, CA 90017 (US).

(21) International Application Number:
PCT/US2009/040568

(81) Designated States (unless otherwise indicated, for every kind of national protection available): AE, AG, AL, AM, AO, AT, AU, AZ, BA, BB, BG, BH, BR, BW, BY, BZ, CA, CH, CN, CO, CR, CU, CZ, DE, DK, DM, DO, DZ, EC, EE, EG, ES, FI, GB, GD, GE, GH, GM, GT, HN, HR, HU, ID, IL, IN, IS, JP, KE, KG, KM, KN, KP, KR, KZ, LA, LC, LK, LR, LS, LT, LU, LY, MA, MD, ME, MG, MK, MN, MW, MX, MY, MZ, NA, NG, NI, NO, NZ, OM, PG, PH, PL, PT, RO, RS, RU, SC, SD, SE, SG, SK, SL, SM, ST, SV, SY, TJ, TM, TN, TR, TT, TZ, UA, UG, US, UZ, VC, VN, ZA, ZM, ZW.

(22) International Filing Date:
14 April 2009 (14.04.2009)

(25) Filing Language: English

(26) Publication Language: English

(30) Priority Data:
61/044,615 14 April 2008 (14.04.2008) US

(71) Applicant (for all designated States except US): HUNTINGTON MEDICAL RESEARCH INSTITUTES [US/US]; 734 Fairmont Avenue, Pasadena, CA 91105 (US).

(84) Designated States (unless otherwise indicated, for every kind of regional protection available): ARIPO (BW, GH, GM, KE, LS, MW, MZ, NA, SD, SL, SZ, TZ, UG, ZM, ZW), Eurasian (AM, AZ, BY, KG, KZ, MD, RU, TJ, TM), European (AT, BE, BG, CH, CY, CZ, DE, DK, EE, ES, FI, FR, GB, GR, HR, HU, IE, IS, IT, LT, LU, LV, MC, MK, MT, NL, NO, PL, PT, RO, SE, SI, SK, TR),

(72) Inventor; and
(75) Inventor/Applicant (for US only): BHATTACHARYA, Pratip [IN/US]; 130 South Michigan Ave., Apt. 1, Pasadena, CA 91106 (US).

[Continued on next page]

(54) Title: METHODS AND APPARATUS FOR PASADENA HYPERPOLARIZATION

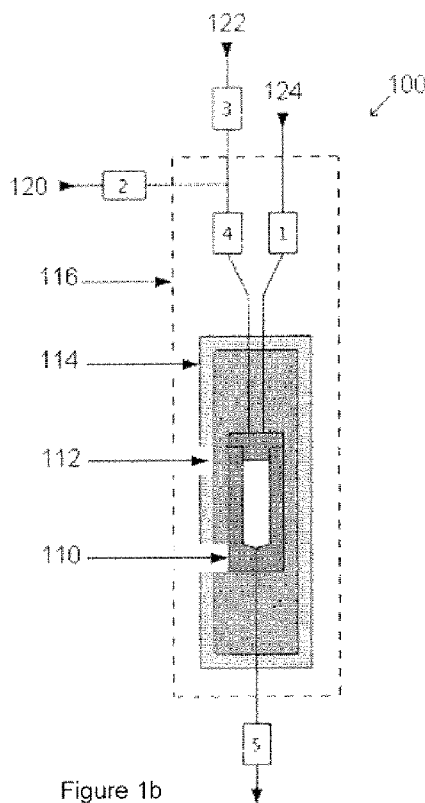


Figure 1b

(57) Abstract: The present subject matter relates to methods and apparatus for a PASADENA polarizer capable of delivering 2.5 - 5 ml of highly hyperpolarized biological ¹³C and ¹⁵N imaging reagents in less than one minute, and capable of repeated delivery every 5 - 8 minutes. Tailored quality control sequences make the subject matter method and apparatus versatile for a variety of biomolecules, capable of undergoing reaction with parahydrogen necessary for effective PASADENA. The subject matter simplifies the technology for routine liquid state generation of hyperpolarized molecules for ¹³C and ¹⁵N subsecond imaging and spectroscopy in vivo and further advance the clinical application of this technology.

WO 2009/129265 A1

WO 2009/129265 A1 

OAPI (BF, BJ, CF, CG, CI, CM, GA, GN, GQ, GW, ML, MR, NE, SN, TD, TG). **Published:**

— *with international search report (Art. 21(3))*

METHODS AND APPARATUS FOR PASADENA HYPERPOLARIZATION

RELATED APPLICATIONS

This application claims the benefit of U. S. Provisional Application Serial Number 61/044,615 filed on April 14, 2008, the entire disclosure and content of which is hereby incorporated by reference in this application.

FIELD OF THE SUBJECT MATTER

The field of the subject matter relates to methods and apparatus for imaging biological subjects by magnetic resonance imaging. More specifically, the present subject matter teaches methods and apparatus for biological imaging utilizing PASADENA hyperpolarization.

BACKGROUND OF THE SUBJECT MATTER

All publications cited herein are incorporated by reference to the same extent as if each individual publication or patent application was specifically and individually indicated to be incorporated by reference. The following description includes information that may be useful in understanding the present invention. It is not an admission that any of the information provided herein is prior art or relevant to the presently claimed invention, or that any publication specifically or implicitly referenced is prior art.

Magnetic resonance imaging ("MRI") is a commonly-accepted technique used in medical imaging to visualize the structure and function of the body and provide detailed images in any plane. In MRI, a scanner creates a powerful magnetic field which aligns the magnetization of hydrogen atoms in a biological subject. Radio waves are used to alter the alignment of this magnetization, causing the hydrogen atoms to emit a weak radio signal which is amplified by the scanner. This technology is useful in connection with disease diagnosis and prognosis, and in the broader study of biological systems. Indeed, many hospitals and medical facilities have MRI imaging equipment on-site, and routinely make use of it to aid in the diagnosis and monitoring of an array of diseases and physiologic conditions. However, as MRI technology has progressed very little there remains a strong need

in the art for improvements in MRI methods and apparatus, specifically improvements in image quality and reproducibility.

Several promising methods of improving nuclear magnetic resonance ("NMR") signal, including high field, rapid gradients, parallel R.F. excitation and acquisition, super-cooled R.F.-coils, rapid imaging and magnetization transfer sequences, as well as paramagnetic contrast agents, have been proposed and researched. However, these methods all operate within the constraints of Boltzman distribution and therefore can only provide incremental improvements in the signal to noise ratio ("SNR") in MRI, varying from 2 -10 fold [J.H. Gillard, A.D. Waldman, and P.B. Barker, *Clinical MR Neuroimaging: Diffusion, Perfusion and Spectroscopy*, Cambridge University Press, New York, NY, 2005].

However, a family of hyperpolarization techniques exist which address the issue of low SNR by developing polarization several orders of magnitude greater than that predicted in the Boltzman equation, and by using a variety of physical and chemical methods to approach polarization of unity ($P = 100\%$). Hyperpolarized noble gas imaging has been practiced by scientists and clinicians for over ten years with great success. The use of xenon gas has been in use by clinicians for two or more years [M.S. Albert, G.D. Cates, B. Driehuys, W. Happer, B. Saam, C.S. Springer, and A. Wishnia, *Biological Magnetic-Resonance-Imaging Using Laser Polarized Xe-129*. *Nature* 370 (1994) 199-201]. Hyperpolarized heteronuclear NMR with ^{13}C and ^{15}N became available for in vivo applications through the systematic improvement and exploitation of dynamic nuclear polarization ("DNP") [J.H. Ardenkjaer-Larsen *et al.*, *Increase in signal-to-noise ratio of > 10,000 times in liquid-state NMR*. *Proceedings of the National Academy of Sciences of the United States of America* 100 (2003) 10158-10163] and parahydrogen-induced polarization ("PHIP") [C.R. Bowers, and D.P. Weitekamp, *Para-Hydrogen and Synthesis Allow Dramatically Enhanced Nuclear Alignment*. *Journal of the American Chemical Society* 109 (1987) 5541-5542]. U.S. Patent No. 6,574, 495 to Golman *et al.*, and U.S. Patent No. 6,872,380 to Axelsson *et al.*, describe apparatus and processes for using PHIP, which is also known as PASADENA (parahydrogen and synthesis allow dramatically enhanced nuclear alignment).

Although PASADENA provides much needed improvement in MRI technology, PASADENA is only utilized in a few laboratories. Cost factors combined

with the operational complexity of current PASADENA apparatus have proven problematic in advancing the technique, which has led to secondary disadvantages including lack of multi-site comparisons and limiting studies to improve on and examine the merits of PASADENA, handicapping further development and propagation of the technique.

The present subject matter is written to overcome this barrier by describing construction of a simple PASADENA polarizer which will provide low-cost access to PASADENA hyperpolarization, allow a systematic comparison between DNP and PASADENA and encourage avenues which appear to offer great promise for in vivo hyperpolarized MRI studies not readily amenable to DNP or hyperpolarized noble gases. In addition, the subject matter describes methods for installing, calibrating and operating the polarizer to optimize PASADENA hyperpolarization. While the ground breaking early discoveries, and some of the subsequent advancements in PASADENA method [Kuhn L.T., Bargon J., *Transfer of parahydrogen-induced hyperpolarization to heteronuclei*. Top Curr Chem 276: (2007) 25–68] required only an NMR spectrometer, an unsaturated molecule and a supply of parahydrogen gas, levels of hyperpolarization reported were generally around 1%, which are insufficient for biological, pre-clinical or clinical studies. Accordingly, a polarizer interface is needed to allow for rapid mixing and chemical reaction of parahydrogen, ^{13}C (or ^{15}N) enriched precursor in a catalyst solution under the correct conditions, within a low field NMR unit. The high spin order inherent in parahydrogen is quantitatively transferred to the precursor, with subsequent generation of the hyperpolarized ^{13}C imaging reagent for injection into an animal or biological test system held within a conventional NMR spectrometer. With the present apparatus, high levels of hyperpolarization permitted early in vivo studies, which proved the potential of hyperpolarized ^{13}C MRI in biology [Golman K, *et al.*, *Parahydrogen-induced polarization in imaging: subsecond C-13 angiography*. Magn Reson Med 46: (2001) 1–5]. Ideally, and within a few minutes, the process is repeated, with the same or very comparable volume and hyperpolarization of the product. The PASADENA polarizer described herein advances upon the prototype described briefly by Axelsson *et al.* [Golman K. *et al.*, *Parahydrogen-induced polarization in imaging: subsecond C-13 angiography*. Magn Reson Med 46: (2001) 1–5] (GE/Amersham, Malmö, Sweden). It is designed to be reliable, low cost and to produce

hyperpolarized biomolecules in solution quickly and efficiently in amounts applicable for biological use. Additionally, unlike previous polarizers, which required the constant attention of 4–5 dedicated and highly trained individuals and was variable in its performance, a single person can operate the subject matter apparatus after a single demonstration. Combined with Quality Assurance (“QA”) methods, described herein, the subject matter PASADENA polarizer and methods for using such are shown to provide reproducible hyperpolarization of biomolecules of $P = [15.3 \pm 1.9]\%$

BRIEF DESCRIPTION OF THE FIGURES

Exemplary embodiments are illustrated in referenced figures and tables. It is intended that the embodiments, figures and tables disclosed herein are to be considered illustrative rather than restrictive. The dimensions shown in various figures are in millimeters.

Figure 1a. A picture of the PASADENA polarizer.

Figure 1b. A schematic view of the PASADENA polarizer.

Figure 2a. A schematic view of the PASADENA laminar-flow reaction chamber.

Figure 2b. A picture of the PASADENA laminar-flow reactor.

Figure 3a. A schematic view of the PASADENA B_1 R.F. transmission coil.

Figure 3b. A picture of the PASADENA B_1 R.F. transmission coil.

Figure 4a. A schematic view of the PASADENA solenoid coil.

Figure 4b. A picture of the PASADENA solenoid coil.

Figure 4c. A picture of the complete assembly of the parts described in Figures 2, 3 and 4.

Figure 5. A schematic view of the process control for the PASADENA polarizer.

Figure 6. A schematic view of a parahydrogen unit for the PASADENA polarizer

Figure 7. A diagram representing the quantification of polarization achieved with the PASADENA polarizer.

Figure 8a. A diagram representing the chemistry of PASADENA.

Figure 8b. A diagram representing hydrogenation in the chemistry of PASADENA.

Figure 8c. A diagram representing the hydrogenation reaction cycle of Rhodium based catalyst.

Figure 9. A graph of the data collected to center the frequency of the low field MR-unit of the polarizer.

Figure 10. A graph of the data collected for ^{13}C and ^1H flip angle calibration of the low field MR unit in the polarizer.

Figure 11a. A ^{13}C NMR spectrum of natural abundance succinic acid at pH 7.4.

Figure 11b. A ^{13}C NMR spectra of carboxyl (1, 4- ^{13}C , ~185 ppm) and methylene (2, 3- ^{13}C , ~ 35 ppm) groups at pH 7.4.

Figure 11c. Simulations and measured ^{13}C NMR spectra of carboxyl and methylene groups at pH 2.95.

Figure 12. A graph of the data collected for calibration of the center frequency of the low field MR unit.

Figures 13a-b. Graphs of the data collected for center frequency of the low field MR unit.

Figure 14. Graphs of the data collected for optimization of SUC hyperpolarization yield by two-dimensional optimization of the B_1 flip angles.

Figure 15. A graph of the T_1 measurement of hyperpolarized 1- ^{13}C -succinate- $d_{2,3}$ in D_2O ($T_1 = [40 \pm 2]$ s) and in H_2O ($T_1 = [27 \pm 3]$ s)

Figure 16. A graph of the quantification of polarization.

Figure 17. A graph of the data collected for reproducibility of hyperpolarization.

Figure 18. An in vivo ^{13}C image of rat achieved after close-arterial injection of 1mL of hyperpolarized ^{13}C succinate.

Figure 19. A diagram of molecular cis addition of parahydrogen followed by hyperpolarization of X nucleus (^{13}C or ^{15}N), polarization storage on X nucleus (potentially allowing monitoring of biochemical events on the time scale of minutes) followed by polarization transfer back to more sensitive protons for NMR detection.

Figure 20a. Graph of ^{13}C reference spectrum of 2.8 mL 17M ethanol with 188 mM ^{13}C concentration per site.

Figure 20b. Graph of ^1H NMR spectrum of 2.8 mL 3M sodium ^{13}C -acetate in D_2O .

Figure 20c. Graph of ^{13}C NMR spectrum of hyperpolarized 6.2 mM 1- ^{13}C -succinate- $\text{d}_{2,3}$, ^{13}C polarization of 5.5% after being stored for 70 s, $T_1=105$ s, the spectrum is acquired using a 12° excitation pulse.

Figure 20d. Graph of ^1H NMR spectrum of hyperpolarized 6.2 mM 1- ^{13}C -succinate- $\text{d}_{2,3}$ where net ^1H signal enhancement is 1,350 fold with 41% spin polarization transfer efficiency.

Figure 20e. Graph of ^{13}C NMR spectrum of hyperpolarized 2.9 mM TFPP. ^{13}C polarization is 9.5% after being stored for 24 s, $T_1=67$ s. The spectrum is acquired using a 12° excitation pulse,

Figure 20f. Graph of ^1H NMR spectrum of hyperpolarized 2.9 mM TFPP where net ^1H signal enhancement is 2,930 fold with 51% efficiency.

Figure 21. Diagram of method towards hyperpolarized proton MR using ^{15}N as a spin storage of hyperpolarization.

Table 1. Shows the components of the fluid control unit.

Table 2. Shows the components of the low field NMR unit.

Table 3. Shows the components of the process control unit.

Table 4. Shows the components of the parahydrogen generator.

Table 5. Shows the corresponding chemicals and axillaries.

Table 6. Shows the workflow of the PASADENA polarizer.

Table 7. Shows the protocol for PASADENA hyperpolarization.

Table 8. Shows the reproducibility and performance of the PASADENA polarizer.

Table 9. Shows the source of materials used in experimental design.

DETAILED DESCRIPTION OF THE SUBJECT MATTER

All references cited herein are incorporated by reference in their entirety as though fully set forth.

Unless defined otherwise, technical and scientific terms used herein have the same meaning as commonly understood by one of ordinary skill in the art to which the subject matter belongs. Singleton *et al.*, Dictionary of Microbiology and Molecular Biology 3rd ed., J. Wiley & Sons (New York, NY 2002); March, Advanced

Organic Chemistry Reactions, Mechanisms and Structure 4th ed., J. Wiley & Sons (New York, NY 1992); and Culbreth L.J., Watson C., Magnetic Resonance Imaging Technology, W.B. Saunders Company (2009), provide one skilled in the art with a general guide to many of the terms used in the present application.

While the description below refers to particular embodiments of the present subject matter, it should be readily apparent to people of ordinary skill in the art that a number of modifications may be made without departing from the spirit thereof, including the use of alternate materials, components, mechanisms, compositions. The accompanying claims are intended to cover such modifications as would fall within the true spirit and scope of the subject matter. All changes that come within the meaning of and range of equivalency of the claims are intended to be embraced therein

The subject matter disclosed herein teaches the subject matter apparatus for PASADENA polarization intended to perform the steps of PASADENA generation, chemistry and hardware of the hydrogenation reaction, and the MRI electronics associated with the spin order transfer. The subject matter further discloses methods for PASADENA hyperpolarization including quality assurance procedures necessary for the setup and optimization of polarization yield, and operational protocols developed for efficient day-to-day operation of the subject matter PASADENA polarizer.

PASADENA Polarizer

The functional components of the polarizer 100 presented are a hydrogenation compartment (laminar flow reaction chamber) 110, a coil to transmit r.f. pulses (B_1) 112, and an electromagnet to generate the static field (B_0) 114 all within a heated chamber 116 (Figure 1a and 1b). A computer interface 130 controls the experimental sequence of fluids and NMR. The entire apparatus is contained in a mobile housing located (7.6 ± 0.1 m) a distance from an unshielded 4.7 T magnet (stray field 0.1 mT). With appropriate r.f. and magnetic field shielding, this distance could be further reduced, with the aim of minimizing the delivery time from the polarizer outlet to the imaging target within the MRI system. A second aspect of the

instrumentation is the parahydrogen generator unit, necessary for the discontinuous production of parahydrogen of high purity (97–100%). This unit can be located off-site, with only sufficient gas held in a transport cylinder on site, for a full day of operation of the polarizer.

Use of a PASADENA polarizer entails rapid mixing and chemical interaction between parahydrogen, a ^{13}C (or ^{15}N) enriched precursor, and a catalyst in the correct proportions in a heated chamber located within a low field NMR spectrometer. The high spin order inherent in parahydrogen is quantitatively transferred to a precursor, with subsequent recovery of the hyperpolarized ^{13}C MR imaging reagent for injection into a biological subject held within a conventional high-field NMR spectrometer [M. Goldman *et al.*, *Design and implementation of C-13 hyperpolarization from para-hydrogen, for new MRI contrast agents*. *Comptes Rendus Chimie* 9 (2006) 357-363]. Such hyperpolarization permitted early in vivo studies which proved the potential of hyperpolarized ^{13}C MRI in biology [K. Goldman *et al.*, *Parahydrogen-induced polarization in imaging: Subsecond C-13 angiography*. *Magnetic Resonance in Medicine* 46 (2001) 1-5; M. Goldman *et al.*, *Hyperpolarization of C-13 through order transfer from parahydrogen: A new contrast agent for MRI*. *Magnetic Resonance Imaging* 23 (2005) 153-157]. Ideally, the process is repeated within a few minutes rendering identical or very comparable results for volume and hyperpolarization of the product. The functional components of the subject matter comprise a laminar flow reaction chamber (reactor), a B_1 coil to transmit radio frequency (R.F.) pulses, and a B_0 electromagnet coil for generating a homogeneous static magnetic field. The B_0 and B_1 coils provide a low-field NMR unit. Tubes and valves are employed for diffusion of the imaging reagents which may be controlled by a computer.

The PASADENA polarizer is contained in a mobile housing cabinet ("Polarizer Cabinet", Figure 1a) located 1 - 10 meters from an unshielded 4.7 T magnet (stray field 0.5mT) of an MR spectrometer. With appropriate R.F. and magnetic field shielding, this distance may be altered, with the aim of minimizing the delivery time from the polarizer outlet to the imaging target within the MR spectrometer. A parahydrogen generator, used for intermittent production of parahydrogen of high (97 – 100%) purity, may be located within close proximity of the mobile housing or

can be located off-site with only sufficient gas held in a transport cylinder on site, for operation of the polarizer.

Referring now to Figure 1b, with ports for fluid control indicated by numbers (1)–(5), a precursor sample 120 (the ^{13}C -enriched precursor-molecule (2) together with the catalyst in aqueous or deuterium solution (3)) is added to the system by injection with compressed nitrogen 122 through a port (4), then transported through clean, sterile plastic tubing by a system of pumps and valves. The precursor sample 120 then resides briefly in a heating coil 116 wound in an ante-chamber and is delivered to a laminar-flow reaction chamber 110. The reaction chamber 110, which has two entry ports (1 and 4) and an outflow port (5), is centered within the B_0 coil 114 and B_1 coil 112 of the low-field NMR. The second reactant, parahydrogen 124, is delivered to the reaction chamber 110 under pressure via port (1). While precursor, parahydrogen 124 and catalyst are held in the reaction chamber 110, a series of pulses played out in the B_1 coil 112 enacts a spin-order transfer sequence specific to the product of the hydrogenation reaction. The hyperpolarized product is ejected from the reaction chamber 110 under the pressure of nitrogen gas 122, filtered to remove the catalyst and injected into an animal, organ or cell preparation previously mounted in the bore of a recording high-field NMR spectrometer. A trigger encoded by the polarizer initiates in vitro or in vivo acquisitions which are completed within $5 \times T_1$ of injection of the hyperpolarized contrast reagent. Each cycle of hyperpolarization is complete in less than 1 minute (52 seconds, Table 6). The entire procedure including hyperpolarization, imaging, rinsing and reloading the polarizer with precursor, occupies 182 seconds (Table 6).

1. Fluid Control Unit:

Valves and Tubing for Fluids

Fluid flow is controlled by electromagnetic solenoid valves connected by polytetrafluoroethylene ("PTFE") tubing and matching nuts with ferrules. A PTFE sleeve was added to the valves to prevent liquids from coming into contact with metal (Table 1). Thus permitting use of acidic reagents.

Ante Chamber

PTFE tubing coiled within a variable heating element capable of reaching 80°C , leads from the injection port to the laminar flow reaction chamber.

Laminar Flow Reaction Chamber

The reaction chamber 110 (in the shape of a right cylinder) is machined from polysulfone plastic to withstand pressure in excess of 15 bar and temperature exceeding 70° C (Figure 2). The reaction chamber consists of three sections, the injection cap, reactor body, and extraction cap, all of which are machined from polysulfone plastic. Both caps are disc-shaped, and include an externally threaded section which mates with a respective internally threaded section in the reactor body. O-rings seal each cap to a respective end of the reactor body. The injection cap includes a central bore for the injection of a stream of liquid precursor solution. The injection cap also includes a laterally offset bore for the injection of nitrogen or parahydrogen. The central bore has a diameter of approximately 0.5 mm, with the diameter of the offset bore being substantially larger. The surface of the inner end of the threaded section of the injection cap is conically shaped to slope down and inward. The surface of the inner end of the threaded section of the extraction cap slopes down and inward to form a funnel-shaped floor, which allows for ejection of the hyperpolarized product through a vertical stepped central bore extending through the extraction cap. The reaction chamber is constructed of plastic to optimize flow and mixing of reagents and gases, as well as to allow rapid evacuation and complete rinsing between each use of the polarizer. Plastic construction also permits repeated use of the polarizer through cycles of extreme pressure and temperature changes without loss of structural integrity. Moreover, in an alternative embodiment, the injection cap or the extraction cap can be formed integrally with the reactor body. Details of the auxiliary equipment, heater, fan, injection port and delivery system are given in Table 1.

2. NMR Unit of the Polarizer:

The purpose of the low-field NMR unit of the polarizer (Figure 3) is to perform the spin order transfer sequence [M. Goldman *et al.*, *Hyperpolarization of C-13 through order transfer from parahydrogen: A new contrast agent for MRI*. *Magnetic Resonance Imaging* 23 (2005) 153-157; M. Goldman, and H. Johannesson, *Conversion of a proton pair para order into C-13 polarization by r.f. irradiation, for use in MRI*. *Comptes Rendus Physique* 6 (2005) 575-581] concurrently with hydrogenation of the precursor molecule with parahydrogen. Accordingly, the coils

for the static (B_0) and R.F. (B_1) fields are located around the laminar flow reaction chamber (Figure 2).

R.F. transmission

Referring now to Figure 3, the B_1 coil consists of two saddle-shaped loops, each with six turns of appropriate gauge magnet wire mounted on opposite sides of a transparent acrylic plastic tube. The two loops are connected in parallel to an r.f. source by flexible leads through a BNC connector in a removable cover on the upper end of the plastic tube. The reaction chamber rests on a movable horizontal annular acrylic disc at the iso-center of the saddle-shaped loops of the B_1 coil. The disc is held in place by screws threaded through the plastic tube and into the edge of the disc, which can be moved vertically to different locations in the tube to accommodate reactors of different sizes. The disc has four outward opening vertical slots to provide clearance for vertical portions of the saddle-shaped loops of the B_1 coil. The two saddle-shaped loops are symmetrically disposed about a common longitudinal access, which also includes the longitudinal axis of the reactor inlet and exit bores.

Static Field

The static magnetic field (B_0) 114 of the low field unit is generated by three separate, vertically stacked, collinear solenoid coils that surround the R.F. transmission (B_1) coil 112 and the reaction chamber 110 (Figure 1 and Figure 5). The (B_1) solenoid coils 112 are driven by a precision DC power supply 132. The center solenoid coil is twice as long as each of the upper and lower coils. The strength and stability of the static field is monitored by a Hall sensor (Probe and Gaussmeter, Space 450, Lake Shore, USA), located between the B_1 coil and the reaction chamber. The sensor is located near the bottom of the reactor, which coincides with the iso-center of the assembly. To allow for independent and precise adjustment of the current flow through each solenoid coil, separate variable power resistors are connected in parallel with each solenoid. This improves low-field homogeneity and compensates for extraneous z gradients, originating from the proximity of the low field unit to the high-field NMR spectrometer, or from other sources in the laboratory.

3. Process Control Unit:

R.F. Transmission (Figure 5)

The R.F. pulses necessary for the spin order transfer are delivered from a synthesizer mounted in the Polarizer Cabinet. Pulses were digitized at an update frequency of 300 kHz, with four sample points per period at the ^1H frequency, and >16 samples per period at the ^{13}C frequency. The signal then passed through a low-pass filter with a cut-off frequency of approximately 150kHz, to an amplifier, and is applied to the un-tuned saddle-shaped loops of the B_1 coil. To facilitate R.F. calibrations, the amplitude of the R.F. output is variable (Table 3). The R.F. optimization is performed as described below. The amplitudes of the square pulses of 25V for carbon and 50V for hydrogen, resulted in pulse widths of 115 μs for an inversion pulse for ^1H , and 230 μs for an inversion pulse for ^{13}C .

Hardware

The analog output of a DAC PXI card is used to generate waveforms of the R.F. sequence. The digital input/output channels of the DAC card is also connected to relays to control opening and closing of the electromagnetic solenoid valves of the fluid system (Table 3).

Software

A custom program on the LabView platform was developed, the main features of which are the control of the digital outputs for mechanized mixing, delivery and recovery of imaging products in the correct sequence and application of a R.F. sequence with precise timing. The R.F. sequence for each experiment is saved in a separate file and reloaded to the program in the form of an ACSII file as necessary.

4. Parahydrogen Generator:

The complete parahydrogen generator is represented diagrammatically in Figure 6, with details of the components listed in Table 4. A similar setup was published by Tam *et al.* [S. Tam, and M.E. Fajardo, *Ortho/para hydrogen converter for rapid deposition matrix isolation spectroscopy*. Review of Scientific Instruments 70 (1999) 1926-1932]. Since the amount of hydrogen to be generated is relatively small, United States safety regulations, which apply to the production of four-hundred (400) or more liters hydrogen, is not applicable to a PASADENA polarizer.

5. Chemicals and Ancillary Equipment:

A clean chemistry laboratory with a ventilation hood is desirable, as is an exhaust route for the gaseous products of the polarizer itself. While parahydrogen itself presents little hazard, reagents, solvents and catalysts employed in PASADENA are associated with a variety of volatile toxins. Table 5 lists the reagents, catalyst and solvents routinely employed. Suppliers are listed in Table 9.

How to prepare chemistry and conduct a hyperpolarization experiment has been described herein under the heading "Quality Assurance."

The subject matter apparatus described herein has been in continuous use providing hundreds of effective hyperpolarizations with several different ^{13}C enriched reagents. Aside from the PASADENA polarizer's facility for use on biological subjects, favorable qualities and components of the subject matter are as follows:

1. The inventive apparatus does not use a metallic nozzle to spray reagent and parahydrogen into the reactor, because it is believed that simple mixing without contact with metals provides greater reproducibility in operation, and removes a cause of contamination and obstruction of flow. Moreover, the elimination of all metallic parts in the reaction chamber and associated conduits accommodates a wider pH range, as needed for certain biologically relevant PASADENA reagents.
2. The power supply is configured such that sufficient power and relatively wide pulses in the SOT sequence are provided; thereby rendering the polarizer function less sensitive to small changes in location and ambient magnetic fields.
3. Control is exercised over the chemistry of PASADENA, with mixing of reagents under nitrogen and better catalysis which results in a more reliable synthesis; thereby removing a source of variability between successive 'runs' of the polarizer.
4. The inventive apparatus is automated; thereby removing the need for multiple operators during a hyperpolarization experiment, easing the path to effective in vitro and in vivo experimentation.

Quality Assurance Procedures

PASADENA is unique in its ability to achieve an extremely high degree of hyperpolarization at liquid state temperatures within seconds all at a relatively low

cost. This is achieved by catalytic addition of molecular parahydrogen to a precursor molecule, while spin order is manipulated consecutively for the generation of net polarization on a designated nucleus, in this case ^{13}C . Nuclear spin polarization characterizes the alignment of spins exposed to a magnetic field, and corresponds to the fraction of all spins that contribute to NMR signal (Eq. 1):

$$P = \frac{N(\uparrow) - N(\downarrow)}{N(\uparrow) + N(\downarrow)} \quad [\text{Eq. 1}]$$

At ambient temperature, the thermal energy exceeds the transition energy of the spin states by orders of magnitude, leaving only ~1-100 ppm of all spins contributing to the overall NMR signal. This is described mathematically by the Boltzmann distribution (Eq. 2):

$$P_{\text{Boltzmann}} = \tanh\left(\frac{\gamma\hbar B_0}{2k_B T}\right) \approx \frac{\gamma\hbar B_0}{2k_B T} \quad [\text{Eq. 2}]$$

(where γ is gyromagnetic ratio characteristic for a nucleus of interest, \hbar is the Plank constant, B_0 is the field strength, k_B is the Boltzmann constant and T is the temperature).

Hyperpolarization techniques hold the potential of increasing polarization to the order of unity, which is an enhancement of 4 – 5 orders of magnitude (η_{observed}) with respect to the thermal polarization originating from the magnetic field (Eq. 3):

$$\eta_{\text{observed}} = \frac{P_{\text{HP}}}{P_{\text{Boltzmann}}} \quad [\text{Eq. 3}]$$

The polarization achieved in total, P_{HP} , provides a measure for the efficiency of the hyperpolarization technique, independent of the specific system for detection. It is predominantly used herein (Eq. 4):

$$P_{\text{HP}} = \eta_{\text{observed}} \cdot P_{\text{Boltzmann}} \quad [\text{Eq. 4}]$$

PASADENA hyperpolarization employs the spin order added to the precursor molecule by addition of parahydrogen to form spin polarization on a third, designated nucleus, such as, but not limited to, ^{13}C or ^{15}N [Kuhn L.T., and Bargon J. *Transfer of parahydrogen-induced hyperpolarization to heteronuclei*. Topics in current chemistry 276: (2007) 25-68].

The two spin $\frac{1}{2}$ system of parahydrogen was predicted in 1924 by Born and Heisenberg [Born M., and Heisenberg W. *The quantum theory of molecules*.

Annalen Der Physik 74: (1924) 1-31], and experimentally measured three years later by Bonhoeffer [Bonhoeffer K.F., and Harteck P. *Experiments on para-hydrogen and ortho-hydrogen*. Naturwissenschaften 17: (1929) 182-182]. The singlet state holds spin zero (Eq. 5), while the triplet states has spin one (Eq. 6).

$$|0,0\rangle = \frac{1}{\sqrt{2}} (|\uparrow\downarrow\rangle - |\downarrow\uparrow\rangle) \quad [\text{Eq. 5}]$$

$$\begin{aligned} |1,1\rangle_1 &= |\uparrow\uparrow\rangle \\ |1,-1\rangle_2 &= |\downarrow\downarrow\rangle \\ |1,0\rangle_3 &= \frac{1}{\sqrt{2}} (|\uparrow\downarrow\rangle + |\downarrow\uparrow\rangle) \end{aligned} \quad [\text{Eq. 6}]$$

The R.F. pulse sequence to form scalar order in the ^{13}C nucleus in a parahydrogenated molecule is described in Goldman *et al.* [M. Goldman, and H. Johannesson, *Conversion of a proton pair para order into C-13 polarization by r.f. irradiation, for use in MRI*. Comptes Rendus Physique 6 (2005) 575-581]. Since the evolution of the spin system is affected by the J couplings characteristic to the molecular environment (Figure 11), the spin order transfer sequence is specific to each individual molecule.

The method has previously been restricted, as early examples were non-biological molecules, soluble only in acetone. A water-soluble molecule which was toxic at the doses employed, and confined to the vasculature after injection in vivo was employed in a demonstration of ^{13}C angiography [K. Golman, *et al.*, *Parahydrogen-induced polarization in imaging: Subsecond C-13 angiography*. Magnetic Resonance in Medicine 46 (2001) 1-5; Mansson S. *et al.*, *C-13 imaging - a new diagnostic platform*. European Radiology 16: (2006) 57-67]. A metabolizable molecule, ^{13}C sodium maleate which is converted to ^{13}C succinate by two hydrogenation steps, has also been reported from this laboratory. In a recent report, we described hyperpolarization of 1- ^{13}C in succinate [Bhattacharya P. *et al.*, *Towards hyperpolarized 13C-succinate imaging of brain cancer*. J Magn Reson, 186: (2007) 108-113; Chekmenev E. *et al.*, *PASADENA Hyperpolarization of Succinic Acid for MRI and MRS*. Journal of the American Chemical Society 130: (2008) 4212-

4213]. Succinate is an intermediate in the tricarboxylic acid cycle and other significant metabolic pathways, including gluconeogenesis [Esteban M.A., and Maxwell P.H. *HIF, a missing link between metabolism and cancer*. *Nature Medicine* 11: (2005) 1047-1048; Rustin P., Munnich A., and Rotig A. *Succinate dehydrogenase and human diseases: new insights into a well-known enzyme*. *European Journal of Human Genetics* 10: (2002) 289-291].

With the advent of imaging reagents with the potential to broaden the use of parahydrogen hyperpolarization in biology, as described above in the subject matter apparatus, comes the need to standardize and automate equipment for this purpose. The following disclosure for the setup and optimization of polarized yield describes in more detail, quality assurance procedures necessary to achieve high levels of ^{13}C hyperpolarization on a consistent basis.

PASADENA is realized in three steps (Figure 8), which determine the overall success of hyperpolarization. First, as source of the spin order, the quality of parahydrogen limits the level of hyperpolarization. Methods for parahydrogen generation are standard and not further discussed herein. Second, is the addition of parahydrogen to the ^{13}C -enriched indicator molecule. Proper chemistry (catalyst) and reaction conditions (hardware) determine whether or not the target molecule is formed efficiently, in such a way that parahydrogen spin order is available for the third step, which entails the manipulations of the spins and transfer of polarization to ^{13}C (^{15}N). Immediately after the hydrogenation reaction, R.F. pulses are applied to form polarization on the designated nucleus in the molecule. Hydrogenation and manipulation of spins by R.F. pulses are carried out within a confined space of a reactor vessel. The reactor vessel is surrounded by coils which provide a static low magnetic field (B_0 coil) and the designed and evolving excitation r.f. pulses (B_1 coil). Design and implementation of low field NMR manipulation is determined by the accuracy with which the quantum mechanical properties of the target molecule (J couplings) is known, and how well the designed manipulations are applied to the spins by R.F. hardware. Presently, the same sequence was used for two ^{13}C molecules of interest. The highly reproducible operation of the PASADENA polarizer and use of $1\text{-}^{13}\text{C}$ Succinate- $\text{d}_{2,3}$, in vitro, described below, demonstrates application in a biological model.

Several of the key metabolites in the urea and choline cycles and neurotransmitter glutamine-glutamate, pathway can be detected and defined by Magnetic Resonance Spectroscopy (MRS) and can be the clinical drivers to ^{15}N hyperpolarization. Hyperpolarizing the metabolites in these cycles can provide invaluable real time biochemical information about the molecular basis of diseases like cancer. For example, choline, synthesized in liver or taken in the diet, enters the brain from systemic circulation via a saturable transport at the blood brain barrier (BBB). The rate of uptake is proportional to blood choline concentration. Once across the BBB, choline enters neurons or glia via active transport. The majority of cellular choline is phosphorylated by choline kinase (CK) and its product phosphoryl choline (PC) is quantitatively the most important metabolite. The rate-regulatory step in choline metabolism is phosphorylcholine conversion to CDP – choline. In normal brain and in glioma, there will be rapid uptake of rapidly infused ^{15}N hyperpolarized choline across the intact BBB, entry into cells and further conversion of choline to phosphorylcholine, via choline kinase. Intracellular accumulation of ^{15}N choline and ^{15}N PC could each reach 0.15 mM in the normal brain after 10 minutes. While free choline, PC and CDP-choline are not distinguishable by PET, the excessive uptake and metabolism of choline will yield signals of significantly different chemical shift in PASADENA/DNP CSI of ^{15}N intermediates.

NMR receptivity scales as γ^3 for spin $\frac{1}{2}$ nuclei. Therefore, direct NMR detection of low g nuclei results in lower signal-to-noise ratio compared to proton detection. As a result, even hyperpolarized ^{15}N spins are inherently $(\gamma_{1\text{H}}/\gamma_{15\text{N}})^2 \sim 100$ fold less sensitive compared to hyperpolarized protons. While protons are better nuclei for detection, short spin lattice relaxation times prevent direct ^1H hyperpolarized MR in biomedical applications.

The present subject matter demonstrates the utility of ^{13}C for spin storage of hyperpolarization followed by ^1H detection using Insensitive Nuclei Enhanced by Polarization Transfer (INEPT) polarization transfer sequence, which theoretically can provide up to $\sim(g_{1\text{H}}/g_{\text{X}})^2$ gain in sensitivity in hyperpolarized biomedical MR (Figure 19). Specifically, the present subject matter hyperpolarized the ^{13}C site of two well studied molecules, 1- ^{13}C -succinate- d_2 and 2,2,3,3-tetrafluoropropyl 1- ^{13}C -propionate- d_3 (TFPP), by PASADENA. Hyperpolarized succinate can be potentially exploited as a metabolic biomarker of cancer, while hyperpolarized TFPP has been shown to be

a specific binder to lipids with a unique chemical shift signature in the lipid bound state potentially useful for plaque and cancer imaging.

The efficiency of the polarization transfer from ^{13}C to ^1H , demonstrated in as 41% (Example 4) for 1- ^{13}C -succinate- d_2 and 50% for TFPP, is a ratio between the ^1H polarization detected after the transfer and ^{13}C polarization as measured by a 12° excitation pulse before the INEPT transfer. While the efficiency of the polarization transfer was 50% or below, hyperpolarized protons are inherently 15.8 fold more sensitive compared to hyperpolarized ^{13}C . As a result, proton detection of hyperpolarized 1- ^{13}C -succinate- d_2 and TFPP increased the overall sensitivity by a factor of 6.5 and 7.9, respectively.

More importantly, using this approach (Figure 21), hyperpolarized ^{15}N MR would become an attractive biomedical and potentially clinical tool due to the much longer spin lattice relaxation time 464 s owing to low γ , but now with the added advantage of more sensitive detection using proton NMR ($\gamma_{215\text{N}} \approx \gamma_{21\text{H}}/100$). In addition, we estimate that ^{15}N hyperpolarization in choline group can be transferred to the nine methyl protons thereby nine spins would be hyperpolarized compared to one ^{15}N per molecule. This could additionally increase the detection sensitivity by factor of nine resulting in overall theoretical signal gain of up to 900 compared to direct detection of hyperpolarized ^{15}N . Furthermore, proton imaging, localized spectroscopy and chemical shift imaging (CSI) will allow improved spatial resolution by $g_{1\text{H}}/g_{\text{X}}$ in each dimension at a given gradient strength.

Specific advantages of ^{15}N NMR can now be exploited by hyperpolarization in the understanding of urea cycle, glutamine-glutamate and choline metabolism *in vivo*. Furthermore, hyperpolarized ^{15}N NMR can have utilized for structure elucidation of proteins and oligonucleotides. Accordingly, the present subject matter shows that: 1) ^{15}N Hyperpolarized MRI and MRS are appealing and feasible; 2) Major advances in SNR and time for imaging has been achieved; 3) Luxury of time: Metabolite flux measurements for 30 minutes or more can be accomplished; and 4) Spin storage: Broadens the approach in case of no nitrogen channel in MR scanners as well as in hyperpolarized conventional ^1H MR.

Table 1 provides the overall quality assurance methods disclosed in the present subject matter for PASADENA hyperpolarization. For convenience, the materials prerequisite (column A) are describe in "Prerequisites for PASADENA," while installation, calibration (column B) and operation of the polarizer (column C) are presented in "Methods for PASADENA."

1. Prerequisites for PASADENA:

Parahydrogen

Commercially available ultra pure hydrogen (Gilmore, South El Monte, USA) was catalytically converted to parahydrogen (pH₂) by slow passage over granular hydrous ferric oxide (IONEX-type O-P catalyst; Molecular Products Inc., Lafayette, CO, USA). After the gas was converted to parahydrogen it was stored in 7 L aluminum cylinders at room temperature at a pressure of 33 bar. The quality of pH₂ was determined to be >97% by high resolution NMR [P. Bhattacharya *et al.*, *Ultra-fast three dimensional imaging of hyperpolarized C-13 in vivo*. *Magnetic Resonance Materials in Physics Biology and Medicine* 18: (2005) 245-256]. Each batch was used within seven days, with no measurable decrease in the yield.

Imaging product precursors

For initial calibration, a previously validated PASADENA reagent, ¹³C HEA, was prepared as an aqueous solution. 2 – 5mg HEA (Isotec, Sigma Aldrich, USA) were dissolved in a small volume of phosphate buffer, pH 7.0, and mixed with the catalyst solution and de-aerated. For further calibration and biomedical studies, 1-¹³C-fumaric acid-d_{2,3} (1-¹³C-FUM-d_{2,3}); (Cambridge Isotope Laboratories, Andover, MA, USA) was dissolved in a small volume of phosphate buffer at pH=2.9. Low pH was necessary for the accurate determination of J-couplings in the resulting hydrogenation product, 1-¹³C succinate (as described further below). The imaging reagent solution was added to the catalyst and alternately exposed to inert gas (N₂) and vacuum. The resulting mixture contained 1-3 mmol/L 1-¹³C-FUM-d_{2,3} and 2.0-2.5 mmol/L catalyst concentrations in 50 mmol/L pH=2.9 phosphate buffer. The aqueous mixture of catalyst and molecular precursor was prepared fresh, prior to each hyperpolarization procedure.

Hydrogenation catalyst

The bisphosphine ligand, 1,4-bis-[(phenyl-3-propane sulfonate) phosphine] butane disodium salt (Q36333, Isotec, OH, USA), was dissolved in H₂O/D₂O to yield 2.5-3.0 mmol/L concentration followed by removal of oxygen using vacuum and nitrogen connected via a manifold. The rhodium catalytic moiety was then introduced to the reaction mixture under N₂ atmosphere as a solution of bis(norbornadiene)rhodium (I) tetrafluoroborate (catalog number 45-0230, CAS 36620-11-8, Strem Chemicals, MA, USA) in acetone with 5% molar excess of bisphosphine ligand with respect to rhodium. The resulting solution was vigorously shaken and acetone was removed under vacuum. Excess of biophosphine is necessary for complete removal of rhodium. The imaging reagent solution was added to the catalyst and alternately exposed to inert gas (N₂) and vacuum. The resulting mixture contained 1–3 mmol/L FUM and 2.0–2.5 mmol/L catalyst concentrations in 50 mmol/L pH 2.9 phosphate buffer. The aqueous mixture of catalyst and molecular precursor was prepared fresh, prior to each hyperpolarization procedure.

The completed PASADENA solution of precursor and catalyst was drawn into a 20 mL plastic syringe and connected to valve 2 of the PASADENA polarizer (Figure 5), for injection of the desired amount of imaging reagent precursor for each experiment (3.5mL unless otherwise noted). When prepared in these proportions, hydrogenation of the precursor was carried to completion and no residual precursor (HEA or 1-¹³C FUM) was detected by ¹³C NMR.

Determination of J-couplings of the PASADENA agents

As indicated in Figure 8, and described in some detail by Bowers [Bowers CR, Weitekamp D. *Transformation of Symmetrization Order to Nuclear-Spin Magnetization by Chemical-Reaction and Nuclear-Magnetic-Resonance*. Phys Rev Lett, 57(21): (1986) 2645-2648], Bargon [Natterer J, Bargon J. *Parahydrogen induced polarization*. Progress in nuclear magnetic resonance spectroscopy 31. 1997: Part 4: 293-315] and more recently by Goldman *et al.* [M. Goldman *et al.*, *Hyperpolarization of C-13 through order transfer from parahydrogen: A new contrast agent for MRI*. Magnetic Resonance Imaging 23 (2005) 153-157; M. Goldman, and H. Johannesson, *Conversion of a proton pair para order into C-13 polarization by r.f. irradiation, for use in MRI*. Comptes Rendus Physique 6 (2005) 575-581], significant

transfer of polarization from parahydrogen to the third nucleus is achieved through design and implementation of a spin transfer sequence which is then applied to the mixture of ^{13}C reagent and rhodium catalyst described previously (Imaging Product Precursors). In order to form ^{13}C hyperpolarization by R.F. radiation, the spin order transfer ("SOT") sequence should be tailored to the J-couplings of the parahydrogen and the nucleus to-be-polarized ($^2J_{\text{CHa}}$, $^2J_{\text{CHb}}$, $^3J_{\text{HaHb}}$).

Quantification of hyperpolarization

A number of strategies have been employed to quantify the extent of hyperpolarization [Association N.E.M. *Determination of signal-to-noise ratio (SNR) in diagnostic magnetic resonance imaging*. NEMA Standards, Publication MS 1-2001 (2001)]. In the present application, the following convention was applied. The signal enhancement (η_{observed}) achieved by hyperpolarization was quantified in respect to the signal of a thermally polarized sample (100% ethanol, 188 mM of natural abundance ^{13}C at each site (Eq. 7)). The signal intensities were determined by numerical integration (xWINNMR software, Bruker Biospin, Germany)

$$\eta_{\text{observed}} = \frac{P_{\text{HP}}}{P_{\text{Boltzmann}}} = \frac{I_{\text{HP}}}{I_{\text{ref}}} \cdot \frac{C_{\text{ref}}}{C_{\text{HP}}} \quad [\text{Eq. 7}]$$

(where I_{HP} , I_{ref} , C_{HP} and C_{ref} are integral intensities and molar concentrations of hyperpolarized and reference samples, respectively).

T_1 decay of hyperpolarization

The decay of ^{13}C polarization caused by longitudinal relaxation (T_1) of the hyperpolarized sample during the delivery to the detection system was determined (Figure 15). This allows for the determination of the nascent signal enhancement (Eq. 8), and nascent level of achieved polarization (Eq. 9).

$$\eta^{t=0} = \eta_{\text{observed}} \cdot \exp\left(-\frac{\text{delivery time}}{T_1}\right) \quad [\text{Eq. 8}]$$

$$P_{\text{HP}}^{t=0} = \eta^{t=0} \cdot P_{\text{Boltzmann}} \quad [\text{Eq. 9}]$$

Unless otherwise indicated, $P_{\text{HP}}^{t=0}$ and $\eta^{t=0}$ are reported in the work presented, using a ^{13}C polarization of $P_{\text{Boltzmann}}=0.00041\%$ or 4.1 ppm at 298K and 4.7T. T_1 values for the PASADENA reagent concerned in calibration and quality assurance ("QA") were determined directly. A series of small angle ($\alpha \approx 8^\circ$) FID experiments was employed to probe the decay of the magnetization of the hyperpolarized agents

(small excitation angle approximation, SEA). The T1 values were extracted by the fit of Equation 10 (Eq. 10) to the data points, taking into account the loss of magnetization caused by the excitation pulses.

$$I(t) = I_0 \cdot e^{-\left(\frac{t}{T_1}\right)} \cdot e^{-\left(\frac{1-\cos(\alpha)t}{TR}\right)} \quad [\text{Eq. 10}]$$

2. Methods for PASADENA

The subject matter method for set-up and calibration of the PASADENA polarizer comprises of seven steps. Together these constitute the quality assurance method which ensures maximum hyperpolarization and optimal reproducibility for each PASADENA reagent.

Step 1. Polarizer fluid control system

An automated fluid control system delivers reagents to the reaction chamber. The steps of the hyperpolarization experiment, including the fluid control system were controlled by custom software (LabView platform, National Instruments, Austin, TX, USA), able to load a R.F. pulse file, and to store the sequence of timings and events in a separate file. The following procedure was optimized to produce hyperpolarized agents in less than one minute, including: (i) Flush the system with N₂ gas (14 bar, valves 3, 4, 5 open), (ii) load the aqueous solution of precursor and catalyst in the N₂ path (valve 2 open) (iii) fill the previously flushed reactor with 10 bar pH₂ and pressurize N₂ path (valves 1 and 3 open), (iv) close pH₂ path, inject precursor solution in pH₂ atmosphere (valves 3 and 4 open) while applying ¹H R.F. saturation pulses (to keep the hydrogen in the singlet state), (v) apply the spin order transfer sequence, and (vi) deliver the hyperpolarized solution to the detector (eg. small animal NMR or clinical MRI scanner) employing residual pressure (valve 5 open).

Step 2. Calibration of the NMR system of the polarizer

An initial calibration of the NMR system of the polarizer is necessary to perform accurate R.F. manipulations on the spins of the PASADENA agent in the reactor. Since the R.F. electronics and coil were designed for transmission only, a

second, external high-field NMR system was employed for the detection (7T Mercury spectrometer, Varian, Palo Alto, USA). A sample of saturated 1-¹³C sodium acetate CH₃-¹³COONa in D₂O was pre-polarized at high field for 3 minutes, delivered to the polarizer for a ¹³C inversion pulse of arbitrary length, followed by delivery back to the high field unit, where the resulting magnetization was detected by a 90° pulse-acquisition.

Step 3. Determine center frequency of NMR system of polarizer

To center the frequency, a ¹³C sample was subjected repeatedly to a "pulse_{polarizer} – delay – pulse-acquisition_{Varian}" experiment while the strength of the low-field in the polarizer was incremented by 0.1mT, and the R.F. was kept constant. The optimal field for the 18 kHz carbon pulse was found to be ~1.76 mT at the position of the Hall sensor of the Gauss meter. Once the optimum field for the carbon frequency was found, the corresponding proton frequency was calculated (75kHz).

Step 4. Thermal flip angle calibration

For the calibration of the flip angles of the R.F. excitation pulses (B₁), the previous protocol for the combination of low-field inversion pulse and high field detection (Figure 9) was employed. At constant B₀, the width of the R.F. pulse given in the polarizer was varied for ¹³C and ¹H frequencies independently. The acquired data was fitted using a T₁ corrected cosine function, providing an estimate for the B₁ fields. The center frequencies of proton and carbon have been aligned in Figure 10 (left). The uncorrected frequencies, or 'true' data are shown in Figure 10 (right).

Step 5. Determination of J-Couplings

While the J-coupling constants for HEP employed in calibration of the polarizer, have previously been reported [M. Goldman, and H. Johannesson, *Conversion of a proton pair para order into C-13 polarization by r.f. irradiation, for use in MRI*. Comptes Rendus Physique 6 (2005) 575-581], the relevant J-couplings for succinate were unknown and were determined by computations employing GAMMA simulations [Smith S.A. *et al.*, *Computer-Simulations in Magnetic-Resonance - an Object-Oriented Programming Approach*. Journal of Magnetic

Resonance Series A 106: (1994) 75-105] and confirmed by experiment [Chekmenev E. *et al.*, PASADENA Hyperpolarization of Succinic Acid for MRI and MRS. Journal of the American Chemical Society 130: (2008) 4212-4213]. The ^{13}C spectra (Figure 11) was acquired using a saturated (100 mM) aqueous solution of succinic acid (natural abundance, Isotec, Sigma Aldrich, USA) with a 14T high resolution spectrometer (Varian, H/C/N probe, 256 acquisitions) without decoupling.

At pH 7.4, substantial line broadening, attributed to chemical proton exchange, was observed on the carboxyl group ($\sim 185\text{ppm}$) which prohibited the resolution of line splitting by J-couplings. All experiments were therefore performed at $\text{pH } 2.95 \ll \text{pKa}$ (Figure 11).

For the simulations, the spectra of a ^{13}C spin coupled to two protons (C, Ha, Hb) was calculated under the effect of Zeemann interaction and indirect couplings ($^2J_{\text{CHa}}$, $^2J_{\text{CHb}}$, $^3J_{\text{HaHb}}$). The simulations were performed iteratively varying the J-couplings until the corresponding experimental spectra (Levenberg-Marquart least-square fit) was found ($^2J_{\text{CHa}} = -7.15 \text{ Hz}$, $^3J_{\text{CHb}} = 5.82 \text{ Hz}$ and $^3J_{\text{HaHb}} = 7.41 \text{ Hz}$).

These constants were programmed for the polarizer and employed to tailor the spin order transfer sequence to the target molecule, $1\text{-}^{13}\text{C}$ succinate-d2,3, during subsequent calibrations.

Step 6. Optimization of spin order transfer: B_0 calibration with Hyperpolarization

Introducing parahydrogen and substituting a PASADENA reagent and catalyst (Section A – Prerequisites for PASADENA) in place of ^{13}C acetate used for calibration, acceptable levels of hyperpolarized signal were achieved as detected in the high-field spectrometer. The optimization of B_0 to center the frequency was repeated over a smaller range, recording the yield of hyperpolarization at each field. Maximal polarization of $P=21\%$ (nominal ^{13}C signal enhancement $\simeq 50,000$) was found at 1.736 mT (Figure 12 left). Polarizer “efficiency” may be assumed “optimum” after the preceding 6 quality assurance steps.

As expected, hyperpolarization was extremely sensitive to deviations from the precise low magnetic field applied during spin order transfer. At $\pm 0.009 \text{ mT}$ from the optimal field, the polarization declined by 50% (FWHM=0.018 mT) (Figure 12 right). Marked variations persisted in the polarization yield at the same field strength

(Figure 13 left), which were attributed to remaining variables in R.F. amplifier performance, reagent preparation technique and, because signal decays rapidly before detection, to prolonged and variable sample delivery times to the spectrometer. Delivering hyperpolarized sample and triggered detection in the NMR scanner were further optimized. The polarizer was moved to the *in vivo* suite, where it was positioned carefully $7.63 \text{ m} \pm 0.5 \text{ cm}$ from a small-animal horizontal bore, high field MRI (4.7T Bruker MRI scanner). An automated system was implemented, whereby the hyperpolarized solution was driven by remaining gas pressure in the reactor, through polyethelene (PE) tubing from the polarizer to an NMR-tube in a dual-tuned $^1\text{H} / ^{13}\text{C}$ solenoid coil in the MR scanner; where after a precise interval (33 seconds) acquisition was triggered. The solution was then drained to permit successive experiments without coil repositioning. Together, these measures proved to be essential for the reliability of the level of achieved polarization, as quantified later. The modifications implemented improved the stability of the B_0 and provided stronger B_1 , allowing for better R.F. performance and less sensitivity of hyperpolarization of HEP to off-resonant B_0 , as demonstrated in Figure 13 (left).

Step 7. B1 optimization with hyperpolarization:

With the goal of *in vivo* application, the next group of calibrations were performed with the non-toxic, water soluble PASADENA biomolecule SUC (Figure 13, right). The hyperpolarization yield was incrementally increased by further optimization of the individual pulse widths of ^{13}C , ^1H in the SOT sequence, at constant B_0 (Figure 14). First, the pulse width of the ^1H pulses in the SOT was varied (Figure 14a). The optimum was determined to be at $115 \mu\text{s}$ (50 V). Next, keeping the ^1H pulse width constant, the experiment was repeated while varying the ^{13}C pulse widths in the SOT sequence (Figure 14b). Each experiment was conducted eight times. The optimum ^{13}C pulse width was $230 \mu\text{s}$ (25 V). Figure 14c demonstrates the multidimensional character of this optimization. The maximal polarization achieved with 1- ^{13}C succinate under these conditions was 18%.

Using these seven quality assurance steps, we defined two important properties of PASADENA for a biologically appropriate molecular imaging reagent in

vitro. First, T_1 of hyperpolarized MRI signal is critical in defining duration of enhanced ^{13}C (or ^{15}N) MRI signal after delivery. We determined the maximum polarization achieved in PASADENA as relevant for quantitative comparison with competing reagents and hyperpolarization techniques. Secondly, the effect of D_2O prolonging the lifetime of polarization is a general property, and of value for most hyperpolarization techniques. The T_1 decay time for HEP was 70s in D_2O , as compared to 50s in H_2O (pH 7, $B_0 = 4.7\text{ T}$).

The relaxation constant of hyperpolarized 1- ^{13}C -succinate-d_{2,3} was determined to be $T_1 = [27 \pm 3]\text{ s}$ ($N=3$, pH 3, $B_0 = 4.7\text{ T}$) in H_2O solvent (at a concentration of 1-3mM of SUC, 2.5mM of catalyst, respectively). $T_1 = [40 \pm 2]\text{ s}$ ($N=4$, pH 3, $B_0 = 4.7\text{ T}$) was significantly prolonged when measured in D_2O (Figure 15). Preliminary results indicate a further increase in measured T_1 , to $\sim 50\text{s}$, when the hyperpolarized reagent-catalyst mixture was buffered to physiological pH 7 immediately before detection (not shown). The effect of D_2O was found to be a general property of hyperpolarization; for example T_1 decay time for HEP was found to be 70s in D_2O , as compared to 50s in H_2O .

Discussion

A reliable, affordable apparatus and methods for hyperpolarization of a biomolecule for routine applications in bio-medical research is presented herein. The performance is demonstrated on 1- ^{13}C -SUCC-d_{2,3}, a ^{13}C PASADENA metabolic agent with the potential to diagnose brain cancer [Chekmenev E. *et al.*, *PASADENA Hyperpolarization of Succinic Acid for MRI and MRS*. Journal of the American Chemical Society 130: (2008) 4212-4213]. This molecule was polarized to an average of $P_{HP}^{I=0} = [15.3 \pm 1.9]$ in 16 experiments, corresponding to an 49,000 fold enhancement at 4.7 T.

The robust design of the polarizer, reflected in the achieved levels and reproducibility of polarization, qualifies (after reagent-sterility is confirmed) for routine bio-medical/clinical application. Three major factors govern both the reproducibility and level of polarization achieved by PASADENA: (A) The primary source of spin order, parahydrogen ($p\text{H}_2$), (B) the hydrogenation of the precursor molecule, and (C)

the manipulation of the spins in the hydrogenated molecule to generate a net polarization (by R.F. Spin order transfer sequence, SOT).

(A) The parahydrogen is routinely enriched to >97%, thereby guaranteeing an excellent source of spin order. It proved to be important to allow a minimum of six hours for the cryo-system to cool down, prior to the generation of pH₂.

(B) It was noted that an inert atmosphere was a key aspect in the preparation of the PASADENA precursor solution. This is attributed to the sensitivity of the Rhodium (Rh) based catalyst to oxygen and moisture. Therefore, bis(norbornadiene)rhodium (I) tetrafluoroborate should be used fresh and with minimum air and light exposure during the chemical preparation of the catalyst solution. An automated setup under inert atmosphere would be desirable to minimize the exposure of the Rhodium catalyst to atmospheric oxygen, accelerate the preparation process and reduce experimental variability. The duration of the hydrogenation reaction may hold further potential for improvements, as preliminary results indicate. This may be attributed to the progress of the hydrogenation reaction, and the loss of spin order state of molecular and bound parahydrogen while the reaction is going on. However, the hydrogenation reaction was deemed to be complete to >99% within 4s under 10 bar pH₂ and 62°C, which is supported by the fact that no precursor signal was found in high field NMR spectrum of the hydrogenated sample.

(C) This leaves the spin manipulations by R.F. to explain why the theoretical value of unity, >90%, ¹³C polarization was not achieved. The pattern of the spin manipulations tailored to the molecule, and how it is realized by NMR electronics, are essential to achieving hyperpolarization. While the first requires knowledge of the coupling constants of the target molecule, the latter is mostly governed by experimental imperfections of the setup.

The static field of the 4.7 T MR unit used for the detection of hyperpolarization was found to perturb the relatively low field in the PASADENA polarizer. At a distance of ~ 7.6 ± 0.1 m, the stray field of the 4.7 T adds a ~ 0.1 mT horizontal component to the vertical 1.7 mT field of the polarizer. This effect is manifested in a complete loss of hyperpolarization if the polarizer is moved into close proximity of the non-shielded magnet. To avoid thermal drift of the B₀ field, a minimum of 4 hours was allowed for the polarizer to reach operational temperature (62° C).

The sensitivity of the hyperpolarization towards fluctuations in B_0 could be reduced by the application of even stronger B_1 pulses. However, possible limitations arise: first, large (with respect to B_0) B_1 fields could make the pulse sequence perform sub-optimally as conventional NMR theory was used for the development (approximation $B_0 \rightarrow B_1$). Second, at strong B_1 , interaction of ^{13}C and ^1H has to be taken into account: There is increased cross-talk between the two, and the pulses applied at one Larmor frequency may affect the spins at the other. Moreover, ^2H nuclei present in the SUC may be affected by the R.F. pulses as well, a matter not yet investigated in detail. Preliminary simulations suggest that the cross-talk between the two channels can be as large as 9% under the conditions of the present study. These challenges may be significantly alleviated by (1) conducting the hyperpolarization experiment at a higher field (~ 10 mT) and/or (2) design of shaped pulses for selective excitation at low field.

Conclusion

Methods and apparatus for a semi-automated PASADENA polarizer capable of delivering 2.5 – 5 ml of highly hyperpolarized biological ^{13}C imaging reagents in less than one minute, and capable of repeated delivery every 5 – 8 minutes, has been achieved and disclosed. The performance of the apparatus is demonstrated on 1- ^{13}C -SUCC- $\text{d}_{2,3}$, an intermediate of the TCA cycle. In 16 experiments, an average polarization of $P_{III}^{I=0} = [15.3 \pm 1.9] \%$ was achieved. Tailored transfer sequences make the PASADENA polarizer versatile for a variety of biomolecules, capable of undergoing reaction with parahydrogen necessary for effective PASADENA. Together these descriptions simplify the technology for routine liquid state generation of hyperpolarized molecules for ^{13}C and ^{15}N subsecond imaging and spectroscopy in vivo and further advance the clinical application of this technology.

While the unique chemical specificity of nuclear magnetic resonance holds great potential in bio-medical research, it is limited by the inherently low polarization (order of 10^{-5}) to in-vivo detection of major metabolic events (\sim mM). Routinely available PASADENA hyperpolarization allows the characterization of metabolic events involving less prevalent metabolites in the micro or even nanomolar range.

EXAMPLES

Example 1

The bisphosphine ligand, 1,4-bis-[(phenyl-3-propane sulfonate) phosphine] butane disodium salt was dissolved in H₂O/D₂O to yield 2.5-3.0 mmol/L concentration, followed by removal of oxygen using vacuum and nitrogen connected via a manifold. A rhodium catalytic moiety was then introduced to the reaction mixture under N₂ atmosphere as a solution of bis(norbornadiene) rhodium (I) tetrafluoroborate in acetone with 5% molar excess of bisphosphine ligand with respect to rhodium. The resulting solution was vigorously shaken and acetone was removed under vacuum (Solution B). For demonstration of hyperpolarization, a readily available, but toxic PASADENA reagent, hydroxyethyl acrylate 1-¹³C (99%), 2, 3-d (98%), ("HEA"), was prepared as an aqueous solution, 2 – 5 mg HEA and dissolved in a small volume of phosphate buffer, pH 7.0, mixed with the catalyst solution and de-aerated by application of a vacuum through a Schlenk line (Solution A). The completed PASADENA solution of precursor and catalyst was drawn into a 20 mL plastic syringe and connected to valve 2 of the PASADENA polarizer (Figure 5), to allow the injection of a desired amount of imaging reagent for each experiment. When prepared in these proportions, hydrogenation of the precursor was carried to completion until no residual precursor (HEA) could be detected by ¹³C NMR.

Example 2

Quantification and Reproducibility of Polarization

Repeated hyperpolarization experiments of 1-¹³C-SUCC-d_{2,3} in D₂O were carried out to determine the level and stability of the polarization produced by the PASADENA polarizer. A representative ¹³C spectrum of hyperpolarized ¹³C-SUCC-d_{2,3} is demonstrated in Figure 16a. Peak amplitude was quantified by comparison with the spectrum of ethanol (Fig 16b), using the equations described herein.

Polarization of ¹³C succinate in D₂O achieved 19%, corresponding to an overall enhancement of 47,000 fold at 4.7 Tesla. To define the reproducibility of polarization, 28 further studies were performed. Note that since each experiment takes only 2 – 3 minutes, with allowance for rinsing and reloading of the polarizer,

the automated polarizer permitted as many as 10 PASADENA hyperpolarizations each hour. Studies in H₂O (N=12) (not shown) and in D₂O (N=16) (Table 8) were performed. Hyperpolarization $P_{HP}^{t=0} = [15.3 \pm 1.9] \%$ was reproducibly achieved in 16 hyperpolarization experiments on 1-¹³C-SUCC-d_{2,3}, in H₂O before the B1 calibration had been completed (Table 8).

Greater reproducibility and higher absolute polarization were achieved after B1 calibration and when the procedure was performed in D₂O (Table 8). Detailed results are presented graphically in Figure 17. The average polarization achieved in D₂O, calculated from T1 to be that at the point of production, was $P_{HP}^{t=0} = [12.8 \pm 3.1\%]$ on 1-¹³C-SUCC-d_{2,3} (2-5 mM) for 16 experiments in four series. The intra day variability was found to be (1) $P_{HP}^{t=0} = [16.5 \pm 3.3] \%$, N=3, (2) $P_{HP}^{t=0} = [15.9 \pm 2.0] \%$, N=4, (3) $P_{HP}^{t=0} = [14.8 \pm 0.1.3] \%$, N=5, (4) $P_{HP}^{t=0} = [15.9 \pm 0.2.0] \%$. This corresponds to a relative enhancement of $\eta^{t=0} = 37,400 \pm 4,600$ at 4.7T. More relevant to the conduct of experiments was the degree of hyperpolarization at the point of measurement. As expected with a mean delay of 33 seconds for delivery and T1 = 27 to 40 seconds, enhancement was significantly lower = $5.4 \pm 1.3\%$ in water and $6.4 \pm 0.8\%$ in D₂O (enhancement $\sim 37,4000 \times [6.5/15.3] = 15,900$ fold at the point of measurement).

No effect of the concentration of ¹³C-SUCC-d_{2,3} on the level of hyperpolarization was found over a narrow range of concentrations 1.65 – 2.89 mM (in water) or from 0.96 – 2.93 mM (in D₂O; Table 8).

Example 3

Efficacy of hyperpolarized 1-13C succinate in vivo

Figure 18 demonstrates, in a representative ¹³C image, overlaid on a standard proton image, the efficiency of hyperpolarized reagent for in vivo imaging. After rapid ante-grade injection into the common carotid artery, hyperpolarized ¹³C succinate appeared in the anatomical distribution coincident with the rat brain, as outlined by ¹H MRI.

Various embodiments of the subject matter are described above in the Detailed Description. While these descriptions directly describe the above embodiments, it is understood that those skilled in the art may conceive

modifications and/or variations to the specific embodiments shown and described herein. Any such modifications or variations that fall within the purview of this description are intended to be included therein as well. Unless specifically noted, it is the intention of the inventors that the words and phrases in the specification and claims be given the ordinary and accustomed meanings to those of ordinary skill in the applicable art(s).

While particular embodiments of the present subject matter have been shown and described, it will be obvious to those skilled in the art that, based upon the teachings herein, changes and modifications may be made without departing from this subject matter and its broader aspects and, therefore, the appended claims are to encompass within their scope all such changes and modifications as are within the true spirit and scope of this subject matter. It will be understood by those within the art that, in general, terms used herein are generally intended as "open" terms (e.g., the term "including" should be interpreted as "including but not limited to," the term "having" should be interpreted as "having at least," the term "includes" should be interpreted as "includes but is not limited to," etc.

Example 4

Sensitivity improvement of ^{15}N and ^{13}C hyperpolarized molecular agents

2.4 mL of 6.2 mM 1- ^{13}C -succinate- d_2 was hyperpolarized at the ^{13}C site to 10.7%. Hyperpolarization was then kept on ^{13}C for 70 s. During this time, the polarized sample was transferred from a low magnetic field polarizer operating at 1.76 mT to 4.7 T animal MR scanner. The ^{13}C polarization decayed from 10.7% to 5.5% corresponding to final ^{13}C signal enhancement by a factor of 13,500. Then the refocused INEPT pulse sequence¹⁰ with $\tau_{\text{INEPT}} = 34$ ms and $\tau_{\text{refocus}} = 32$ ms (Figure 19) was used to transfer polarization from ^{13}C to protons within 1- ^{13}C -succinate- d_2 (Figure 20a and Figure 20b). The results indicated that the two protons were successfully hyperpolarized corresponding to 41% polarization transfer efficiency and 1,350 fold ^1H NMR signal enhancement per two methylene protons. In a follow up experiment, 2.4 mL of 2.9 mM TFPP was polarized to 14% and the hyperpolarization was stored on the 1- ^{13}C site for 24 s, during which the polarization decayed to 9.5% corresponding to the final signal enhancement of 23,300 fold at this site (Figure 20e). The delays of the refocused INEPT were $\tau_{\text{INEPT}} = 20$ ms and τ_{refocus}

= 16 ms. The combined intensity of the three NMR lines corresponding to four hydrogen atoms (Figure 20f) was enhanced by a factor of 2,930, corresponding to the 50% polarization transfer efficiency by the refocused INEPT sequence.

Table 1: Fluid Control Unit

Function	Part	Description	Commercial availability
Transport and reaction	Tubing	PTFA tubing	Y ¹
	Valves	Electromagnetic solenoid and manual valves	Y ^{2, 3, 4}
	Ante +- chamber	PTFA tubing	Y ¹
	Reaction chamber	Injection cap, reactor body, end cap	-
Aux	T control	Heater, fan, controller, relay	Y ⁵
	Injection timer	On-delay relay	Y ⁶
	Intake precursor	30ml rubber piston syringe	Y ⁷

Table 2: Low Field NMR Unit

Function	Part	Description	Commercial availability
B1 field	B1 coil	Saddle-shaped coil	-
	Synthesizer	DAC analog-out	Y ⁸
	Amplifier	Audio amplifier	Y ⁹
	Filter	150 kHz low-pass filter	Y ¹⁰
	Monitoring	Oscilloscope	Y ¹¹
	Cables	Coaxial cable RG58	Y ¹²
Bo field	Bo coil	Solenoid coil	-
	Power supply	DC power supply	Y ¹³
	Monitoring	Gauss meter	Y ¹⁴

Table 3: Process Control Unit

Function	Part	Description	Commercial availability
Software	Platform	LabView	Y ¹⁵
	Program	pPASADENA control V1.1	-
Hardware	Synthesizer	DAC analog-out	Y ⁸
	Valve, trigger control	DAC digital-out	Y ¹⁶
		Relays	Y ¹⁷

Table 4: Parahydrogen Generator

Function	Description	Commercial availability
Low T Unit	Helium two stage cold head	Y ¹⁸
	Pressure gauge	Y ¹⁹
	Vacuum shroud	Y ²⁰
	Helium compressor / cryodrive	Y ²³
	Vacuum pump	Y ²⁴
	Valve	Y ²⁵
	Flow limiter	Y ²⁶
	Relay	Y ²⁷
	Pressure display	Y ²⁸
	Water cooler	Y ²⁹
	Tubing connectors	Y ³⁰
	Regulator for H ₂ supply	Y ³¹
	Tubing at ambient T	Y ³²
Flow meter	Y ³³	
Catalytic converter	Low T conversion container	Y ³⁴
	Catalyst	Y ³⁵
Storage	Cylinder	Y ³⁶

Table 5: Chemicals and Anxillary

Function	Part	Description	Commercial availability
Chemicals	Precursor	1- ¹³ C FUM-d2,3, 1- ¹³ C HEA-d2,3	Y ^{37, 38}
	Catalyst	Rh-complex and ligand	Y ^{39, 40}
	Solvent	D2O, H2O, buffer	Y ⁴¹
Aux Lab Equipment		Schlenk line with vacuum, N ₂ , in fume hood	Y ⁴¹
		Glass ware	Y ⁴¹
		Precision scale	Y ⁴¹

Table 6. Workflow of the PASADENA experiment. Automated software controls the time sensitive steps.

(a) Event Nr.	(b) Time point	(c) Description	(d) Duration
<i>Manual preparation / Manual control</i>			
1	0 s	Clean polarizer: <i>Flush lines and reactor with 14 b N2 gas (Valve V2, V3, V4, V5).</i>	10 s
2	10 s	Preheat precursor solution: <i>Transfer 3.5mL of precursor into the injection line (V2).</i>	120s
Total time for preparations: 130 s			
<i>Automated procedure / computer control / Automated sequence</i>			
1	0 s	<i>Fill reaction chamber with pH2 (V1).</i>	10 s
2	10 s	Hydrogenation reaction: <i>Inject the precursor into the reactor (V3, V4).</i> <i>Apply R.F. 1H decoupling sequence.</i>	3 s
3	13 s	Hyperpolarization: <i>Apply R.F. spin order transfer sequence.</i>	>1 s
4	14 s	<i>Expel hyperpolarized agent (V5).</i>	2 s
5	19 s	<i>Delivery agent and rest (V5).</i>	28 s
5	52 s	Signal detection: <i>Send trigger signal</i>	3 s
Total time for hyperpolarization: 52s			

Table 7. Protocol for PASADENA hyperpolarization.

A. Prerequisites	B. Setup / Installation	C. Experimental routines
1. Parahydrogen (>95%) 2. Precursor molecule(s) 3. Hydrogenation catalyst 4. PASADENA Polarizer	Setup of polarizer: 1. Fluid control system; 2. Low field NMR system Calibrate low field NMR system: 3. Center frequency ^1H , ^{13}C 4. Flip angles ^{13}C , ^1H 5. J couplings for target molecule Optimize Spin order transfer: 6. B_0 optimization 7. B_1 optimization	1. Flush the polarizer 2. Flush delivery system 3. Prepare 4.7T MRI scanner 4. Check temperature 5. Check gas pressure (N_2 , pH_2) 6. Check B_0 value 7. Check R.F. amplitudes of B_1 pulses

Summary of the minimum requirements for successful hyperpolarization using prototype polarizer. A systematic description of PASADENA methodology follows. Tasks required to establish PASADENA hyperpolarization, optimize the operating equipment and provide quality assurance in daily use are summarized under these headings.

Table 8. Reproducibility and performance of the polarizer:

(A) Number	(B) $P_{HP}^{t=0}$ (%)	(C) $P_{HP}^{t=33s}$ (%)	(D) c (SUCC) (mM)	(E) c (Rh) (mM)	
Day 1	1	15.5	6.5	1.71	2.2
	2	20.1	8.4	1.71	2.2
	3	13.8	5.8	1.71	2.2
Day 1,		$P_{HP}^{t=0} = [16.5 \pm 3.3] \%$			
N = 3:		$P_{HP}^{t=33s} = [6.9 \pm 1.3] \%$			
4	17.1	7.2	1.4	2.2	
5	15.9	6.7	1.4	2.2	
6	17.5	7.3	1.4	2.2	
7	13.0	5.5	0.96	2.2	
Day 2,		$P_{HP}^{t=0} = [15.9 \pm 2.0] \%$			
N = 4:		$P_{HP}^{t=33s} = [7.1 \pm 0.3] \%$			
8	14.9	6.2	2.93	2.1	
9	15.4	6.4	2.93	2.1	
10	16.3	6.8	1.24	2.2	
11	14.7	6.2	1.24	2.2	
12	12.7	5.3	1.24	2.2	
Day 3,		$P_{HP}^{t=0} = [14.8 \pm 1.3] \%$			
N = 5:		$P_{HP}^{t=33s} = [6.5 \pm 0.3] \%$			
13	15.3	6.4	1.59	2.2	
14	14.3	6.0	1.95	2.2	
15	15.1	6.3	1.59	2.2	
16	13.3	5.6	2.07	2.2	
Day 4,		$P_{HP}^{t=0} = [14.5 \pm 0.9] \%$			
N = 4:		$P_{HP}^{t=33s} = [6.2 \pm 0.2] \%$			
Total		$P_{HP}^{t=0} = [15.3 \pm 1.9] \%$			

N = 16 $P_{HP}^{t=33s} = [6.4 \pm 0.8] \%$

- (A) Number of experiment
 - (B) Level of nascent polarization ($T_1=40s$)
 - (C) Level of polarization after 33s
 - (D) Concentration of 1- ^{13}C -SUCC- $d_{2,3}$ in mM
 - (E) Concentration of Rh-catalyst complex in mM
-

Four different sets of experiments of hyperpolarization of 1- ^{13}C -SUCC- $d_{2,3}$, in D_2O were performed as indicated (see also Figure 17).

Table 9. Source of Materials

1	PTFA tubing, OD / ID/ WT: 1/8, 1/16, 1/32 ", Nalgene, NY, USA
2	Two-ways rocker valve, mod. 6126 (id. 431568, for liquids), Burkert Fluid Control Systems, Indelfingen, Germany
3	Addition to 6126 by Promech, Malmö, Sweden
4	Solenoid valve, mod. H22G9DGV (for gases), Peter Paul Co., CN, USA
5	Mod. CN132, Omega Engineering, CN, USA
6	Mod. 814 Syrelec, Crouzet, TX, USA
7	BD, Franklin Lanes, NJ, 07417, USA
8	Mod. PXI 1042, PXI 8331, PXI 6251, National Instruments, TX, USA
9	Mod. 8522 TX, Onkyo, USA
10	Mod. 3200, Krohn Hite, USA
11	Mod. TDS 3012 B 100 MHz 1.25 Gs/s, Tectronix, USA
12	Generic
13	Mod. 3615A, Agilent, USA
14	Gaussmeter 450 with axial probe MMA 2508 VH, Lake shore, USA
15	LabView (V. 8), National Instruments, TX, USA
16	Mod. USB 6501, NI, TX, USA
17	Mod. ER-16, NI, TX, USA
18	Mod. B51907000 6130 cold head assembly, Edwards, MA, USA
19	Active pirani gauge, APG M NW 25 ST/ST, PN: D0217200 SN: 02723484
20	Generic, S.C.B., Herrmann-Cossmann-Str. 19, D-41472 Neuss, Germany
23	3.0kW He cryodrive, Edwards, MA, USA
24	Mod. RV3, with oil mist filter EMF 10, Edwards, MA, USA
25	Mod. LCPV2 5 EKA, Edwards, MA, USA
26	Needle valve HAKE 1315G4s 5000PSI 1345b 1 0553, set 4.5
27	generic, 240V
28	Mod. AGD, set to $\sim 2 \times 10^{-4}$ b, Edwards, MA, USA
29	Mod. Neslab Merlin M150, Thermo Fischer Scientific, MA, USA
30	"Instrumentation-quick-connect" (SS), Swagelok, OH, USA
31	Regulator 250 b to 68 b, Advanced specialty gas equipment, NJ, USA
32	¼ " copper / ¼" SS generic, 7RSW SAE 100 R7-4 ¼ 2750 PSI swagelok, OH,

	USA
33	Mod. 7101 043001A, King Instruments, CA, USA
34	¼ "copper tubing, generic
35	Ionex-Type O-P catalyst (hydrous ferric oxide), Molecular products, CO, USA
36	7 L volume, M25x2 150, CBM produkter AB, Box 47, 131 06 Nacka, Sweden, or P2795z, Luxfer, CA, USA
37	fumaric acid, 1- ¹³ C (99%), 2, 3 -d ₂ (96%), Cambridge Isotope Laboratories, MA, USA
38	hydroxyethyl acrylate 1- ¹³ C (99%), 2, 3, 3, -d ₃ (98%), Isotech, Sigma-Aldrich, MO, USA
39	bis(norbornadiene)rhodium(I) tetrafluoroborate, catalog number 45-0230, CAS 36620-11-8, >96%, Strem Chemicals, MA, USA
40	1, 4-bis[(phenyl-3-propanesulfonate) phosphine] butane disodium salt, Q36333, Isotech, Sigma Aldrich, MO, USA.
41	generic

CLAIMS

WHAT IS CLAIMED IS:

1. An apparatus, comprising:
 - a laminar flow reaction chamber for hyperpolarization;
 - a coil surrounding the laminar flow reaction chamber for transmission of radio frequency (R.F.) pulses;
 - an electromagnet surrounding the coil for generating a static field;
 - a power source for supplying power to the coil and the electromagnet;
 - a series of valves employed for fluid flow and delivery to the laminar flow reaction chamber; and
 - a central processor,wherein said central processor controls said series of valves employed for fluid flow and delivery of an image reagent solution to the laminar flow reaction chamber for hyperpolarization.
2. The apparatus of claim 1, further comprising an image reagent solution source in communication with the laminar flow reaction chamber for supplying the image reagent solution.
3. The apparatus of claim 1, further comprising a parahydrogen generator in communication with the laminar flow reaction chamber for generating and delivering parahydrogen.
4. The apparatus of claim 1, further comprising a nitrogen source in communication with the laminar flow reaction chamber for supplying nitrogen.
5. The apparatus of claim 1, further comprising a Hall sensor for monitoring the strength and stability of the power source.
6. The apparatus of claim 5, wherein the Hall sensor is located between the coil and laminar flow reaction chamber.

7. The apparatus of claim 1, wherein the series of valves are each composed of a material independently selected from a group consisting of polytetrafluoroethylene, perfluoroalkoxy polymer resin, fluorinated ethylene-propylene, fluoropolymer, fluorocarbon, polysulfone and combinations thereof.
8. The apparatus of claim 1, wherein the series of valves are electromagnetic solenoid valves.
9. The apparatus of claim 1, wherein application of the coil and electromagnet in conjunction with mixing, delivery and recovery of the image reagent solution is controlled by the central processor.
10. The apparatus of claim 1, further comprising a synthesizer in communication with the coil for facilitating radio frequency pulse transmission.
11. A method of magnetic resonance imaging, comprising:
 - providing parahydrogen;
 - producing an image reagent solution comprising a catalyst;
 - providing an apparatus, comprising:
 - a laminar flow reaction chamber for hydrogenation;
 - a coil surrounding the laminar flow reaction chamber for transmission of radio frequency (R.F.) pulses;
 - an electromagnet surrounding the coil for generating a static field;
 - a power source for supplying power to the coil and electromagnet;
 - a series of valves employed for fluid flow and delivery; and
 - a central processor,
 - reacting the image reagent solution with the parahydrogen in the laminar flow reaction chamber to form a hyperpolarized product;
 - transmitting R.F. pulses provided by the coil to enact a spin-order transfer sequence in the hyperpolarized product;

ejecting the hyperpolarized product from the laminar flow reaction chamber;
filtering the hyperpolarized product to remove the catalyst;
injecting the filtered hyperpolarized product into a biological subject;
and
exposing the biological subject to a high-field nuclear magnetic resonance spectrometer.

12. The method of claim 11, wherein the imaging reagent solution comprises carbon-13, nitrogen-15, oxygen-18, and combinations thereof.
13. The method of claim 11, wherein the mixing, delivery and recovery of the imaging reagent solution and parahydrogen are controlled by the central processor.
14. The method of claim 11, further comprising optimization of the apparatus by flushing the laminar flow reaction chamber.
15. The method of claim 11, further comprising optimization of the apparatus by initial calibration of the nuclear magnetic resonance spectrometer.
16. The method of claim 11, further comprising optimization of the apparatus by determining a center frequency of the nuclear magnetic resonance spectrometer.
17. The method of claim 11, further comprising optimization of the apparatus by calibrating the radio frequency pulses of the coil.
18. The method of claim 11, further comprising optimization of the apparatus by determining J-couplings for the imaging reagent solution.
19. The method of claim 11, further comprising optimization of the apparatus by calibrating spin order transfer for the electromagnet by hyperpolarization.

20. The method of claim 11, further comprising optimization of the apparatus by calibrating spin order transfer for the coil by hyperpolarization.
21. The method of claim 11, further comprising the use of Inensitive Nuclei Enhanced by Polarization Transfer (INEPT) sequence to transfer hyperpolarized product to proton (^1H).
22. The method of claim 11, wherein the apparatus further comprises a Hall sensor for monitoring the strength and stability of the of the power source.
23. The method of claim 21, wherein the Hall sensor is located between the coil and laminar flow reaction chamber.
24. The method of claim 11, wherein the series of valves in the apparatus are each composed of a material selected independently from a group consisting of polytetrafluoroethylene, perfluoroalkoxy polymer resin, fluorinated ethylene-propylene, fluoropolymer, fluorocarbon, polysulfone and combinations thereof.
25. The method of claim 11, wherein the series of valves in the apparatus are electromagnetic solenoid valves.
26. The method of claim 11, wherein the central processor controls mixing, delivery and recovery of the image reagent solution and application of the coil and electromagnet.
27. The method of claim 11, wherein the apparatus further comprises a synthesizer in communication with the coil for facilitating radio frequency pulse transmission.
28. The method of claim 11, wherein the apparatus further comprises a parahydrogen generator in communication with the laminar flow reaction chamber for generating and delivering parahydrogen.

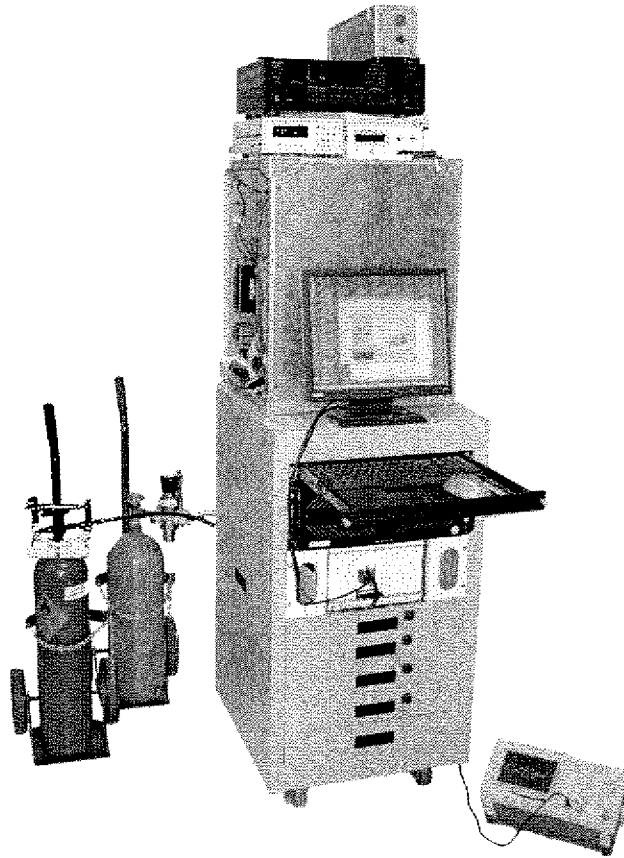


Figure 1a

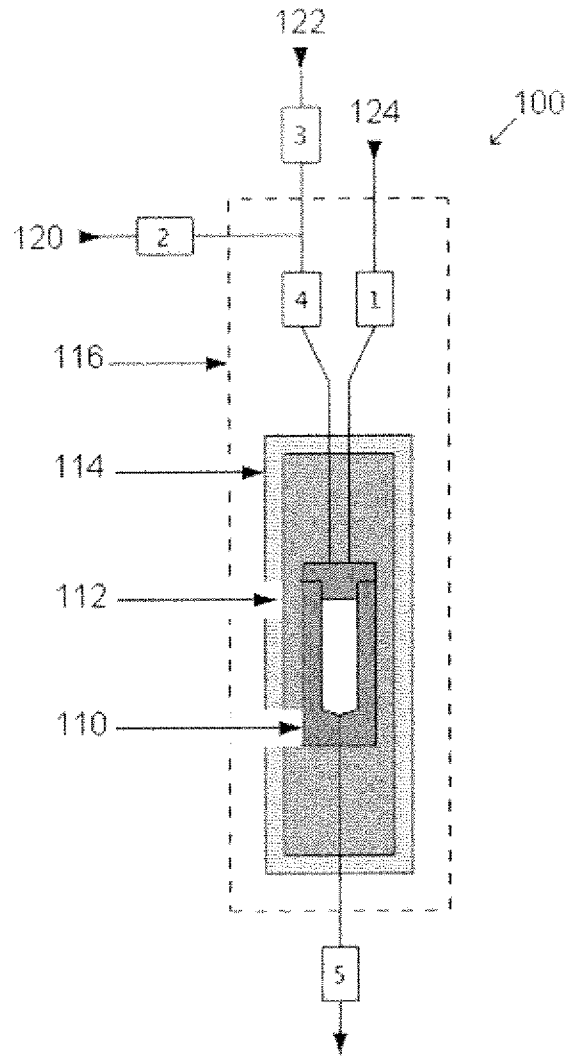


Figure 1b

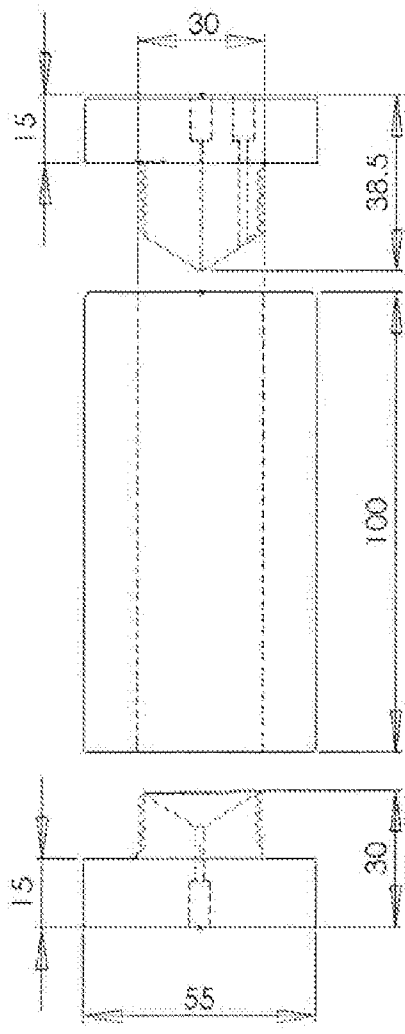


Figure 2a

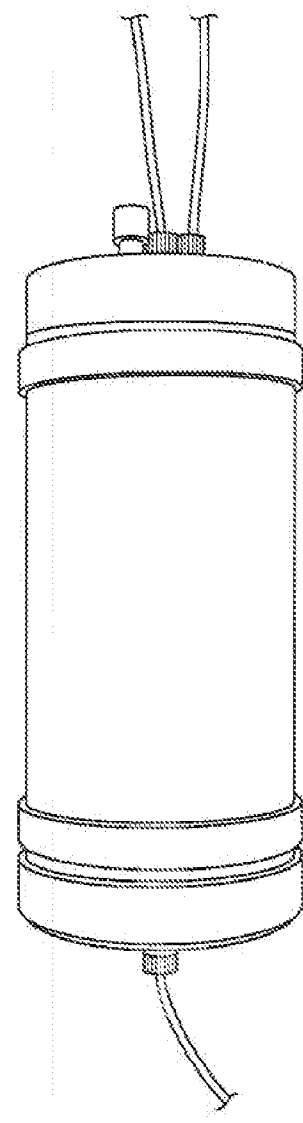


Figure 2b

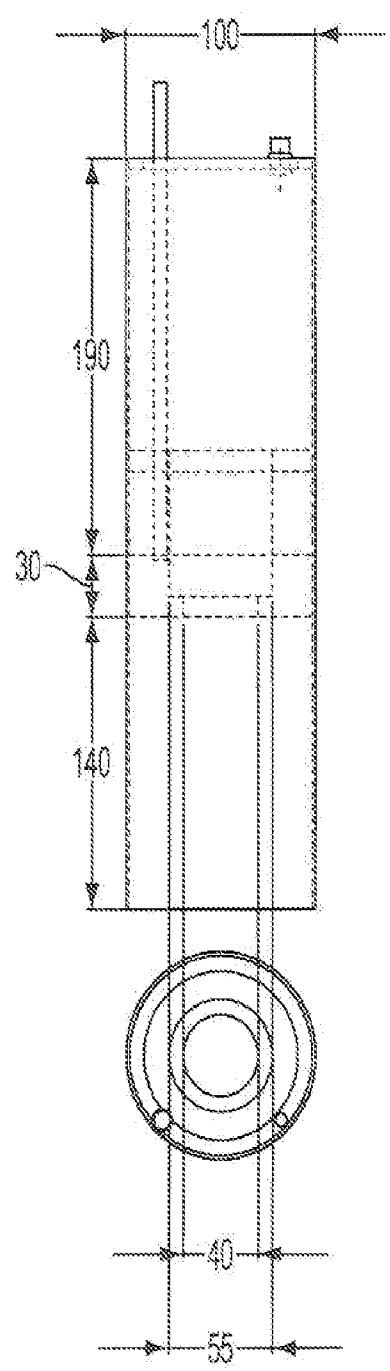


Figure 3a

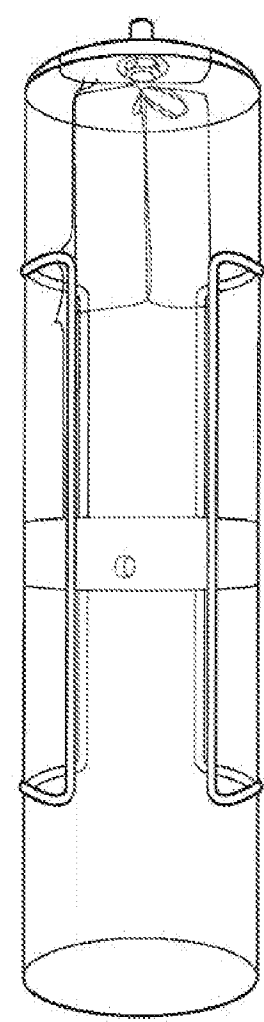


Figure 3b

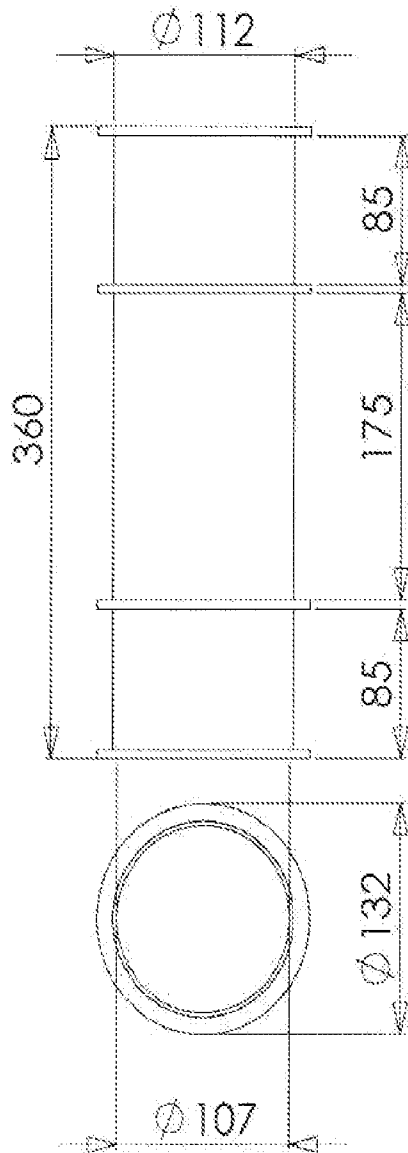


Figure 4a

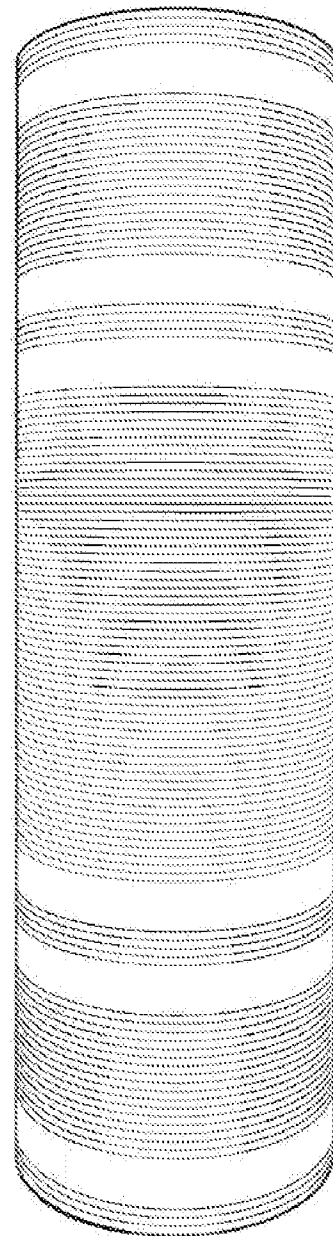


Figure 4b

6/21

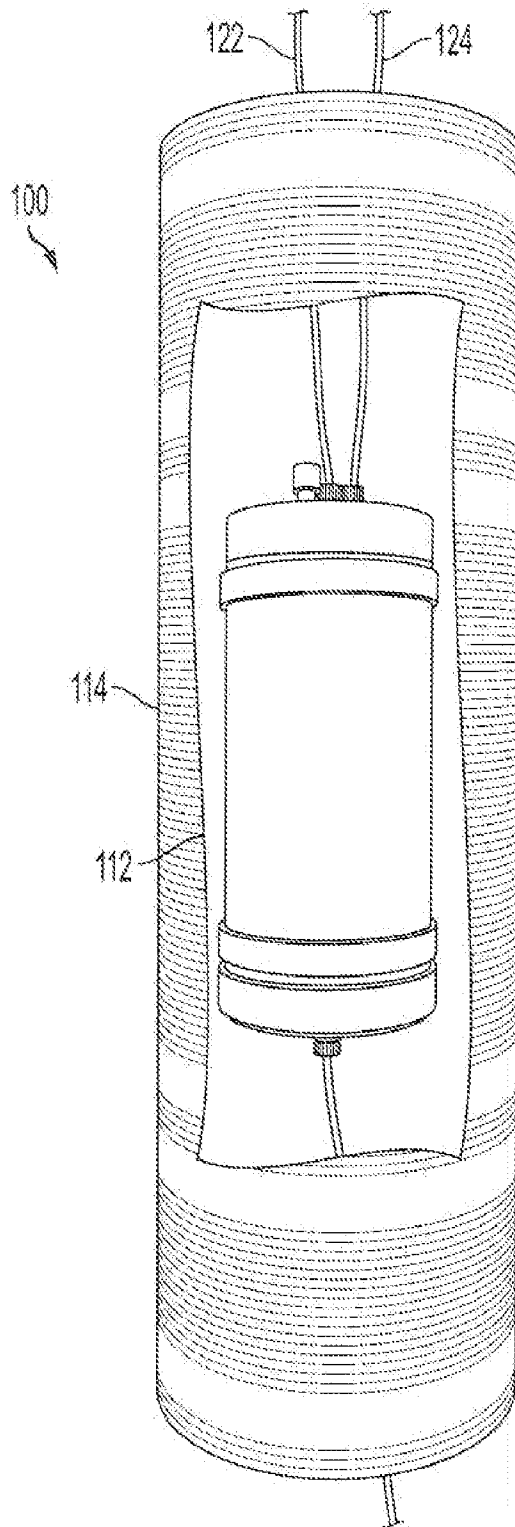


Figure 4c

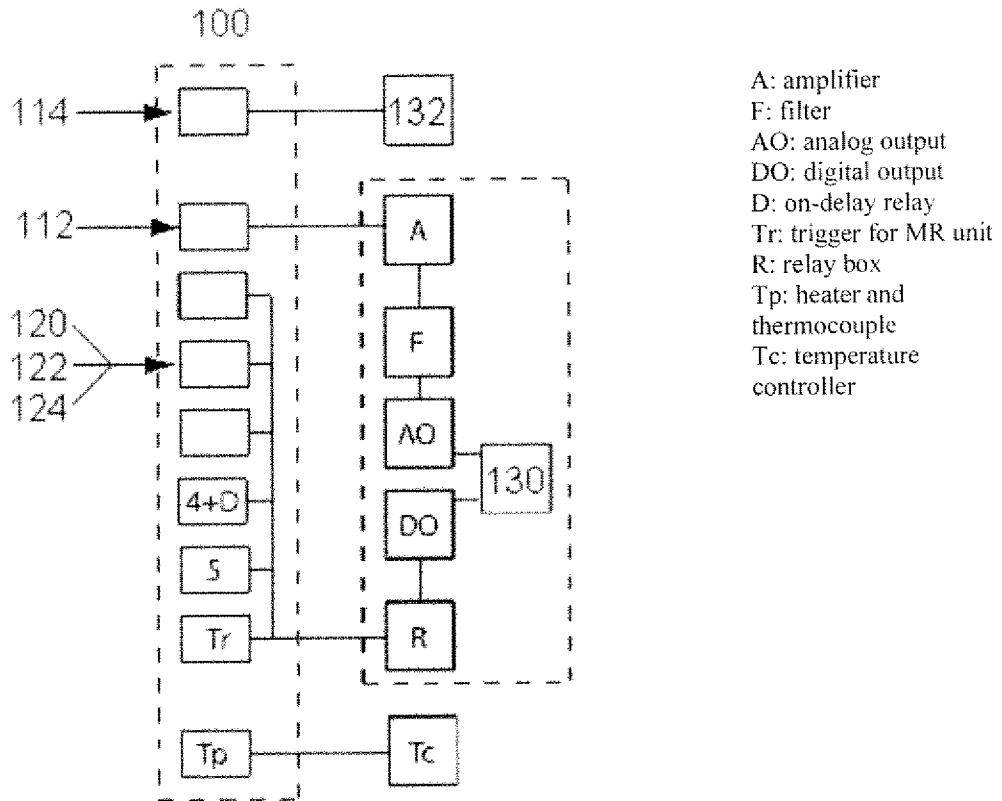


Figure 5

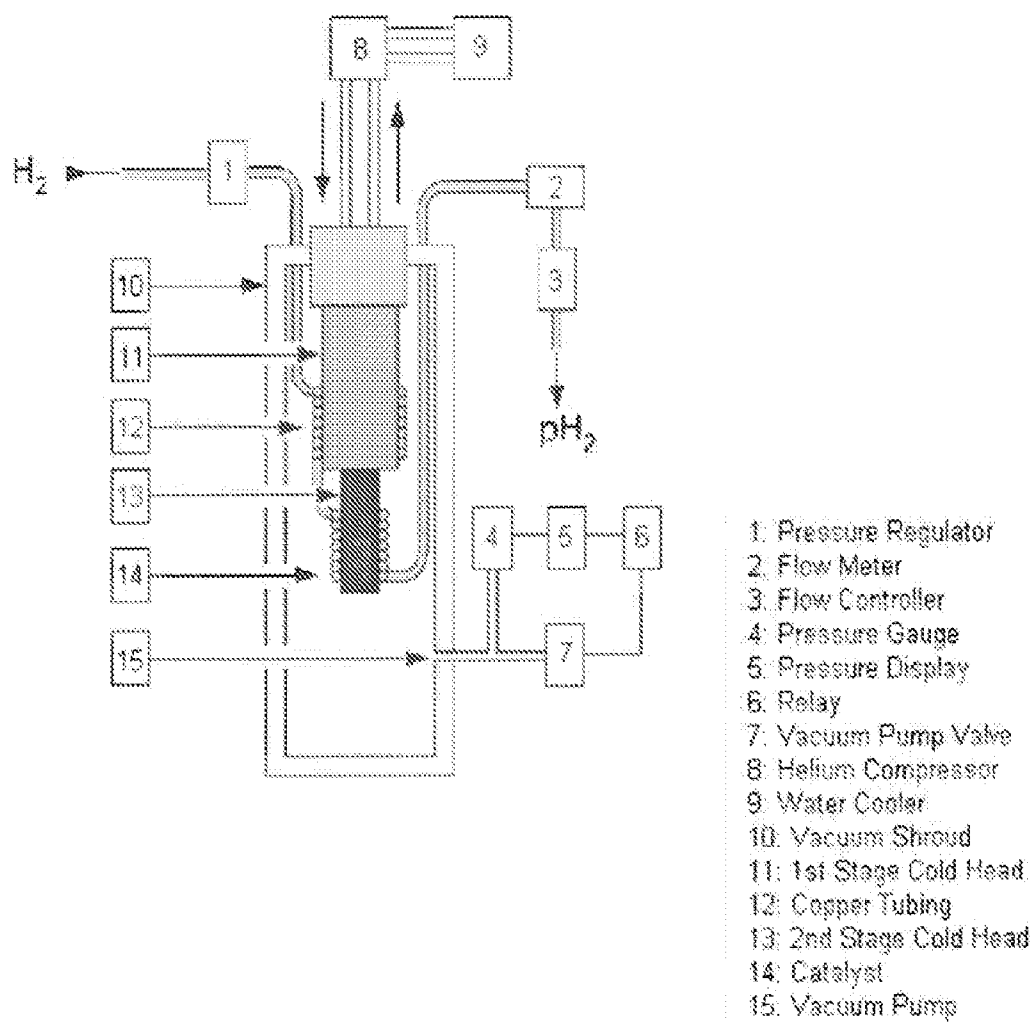


Figure 6

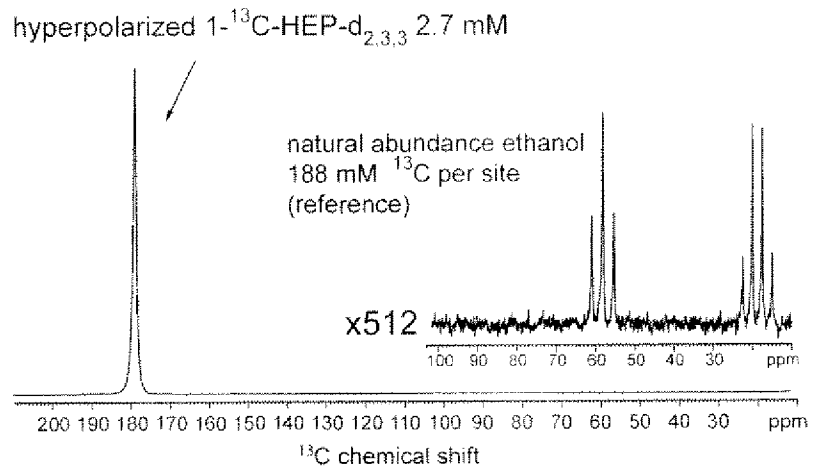


Figure 7

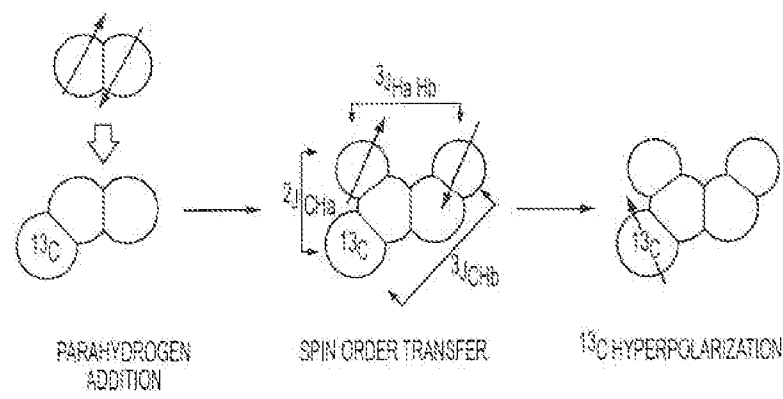


Figure 8a

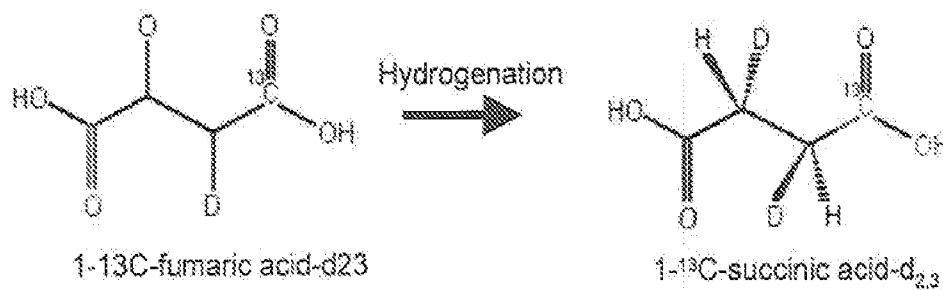


Figure 8b

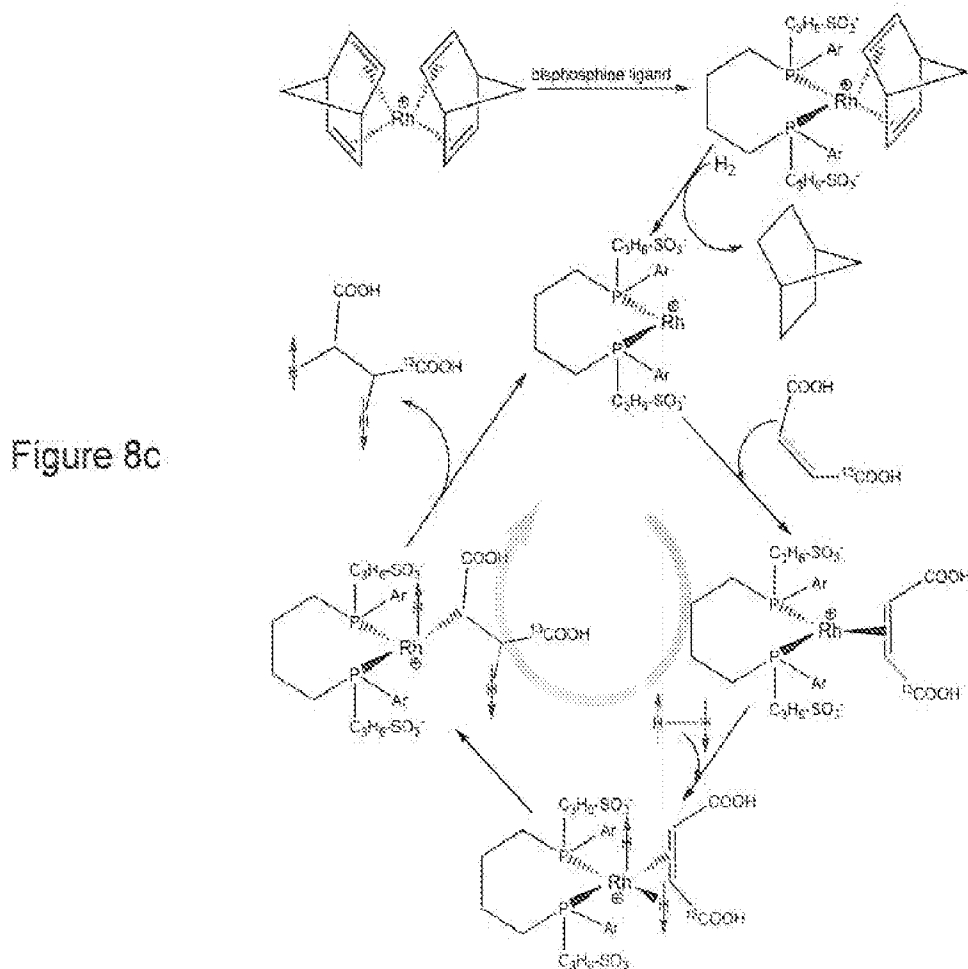


Figure 8c

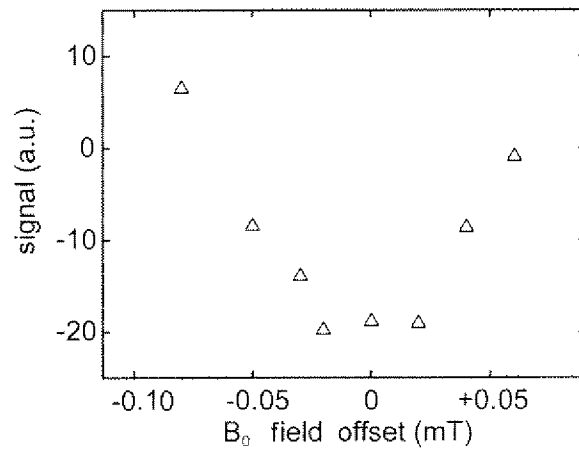


Figure 9

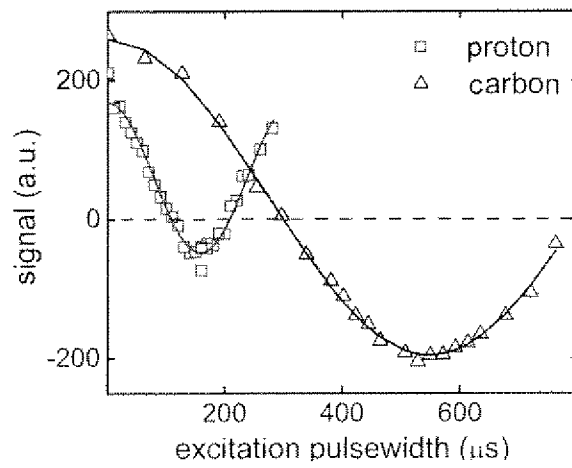


Figure 10

12 / 21

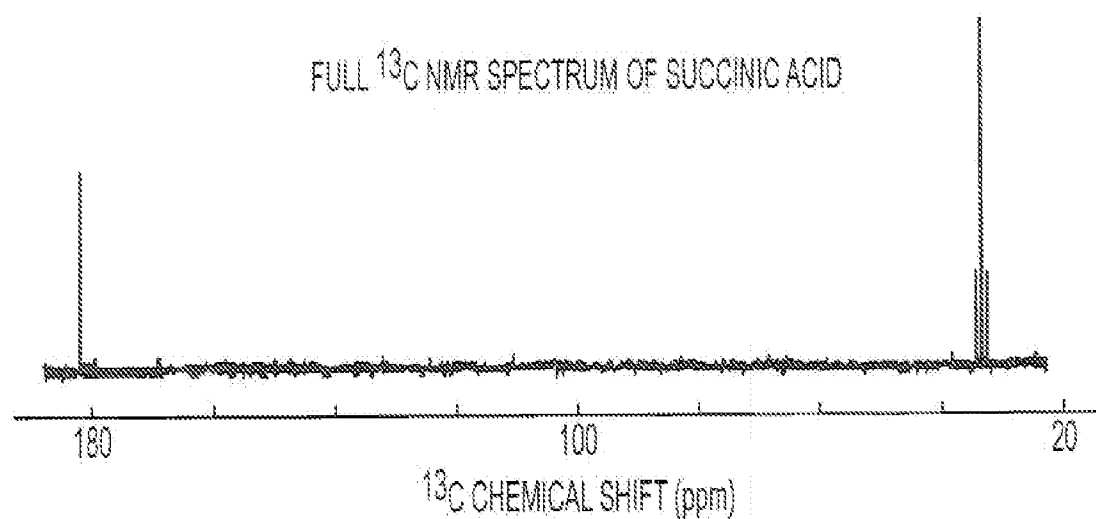


Figure 11a

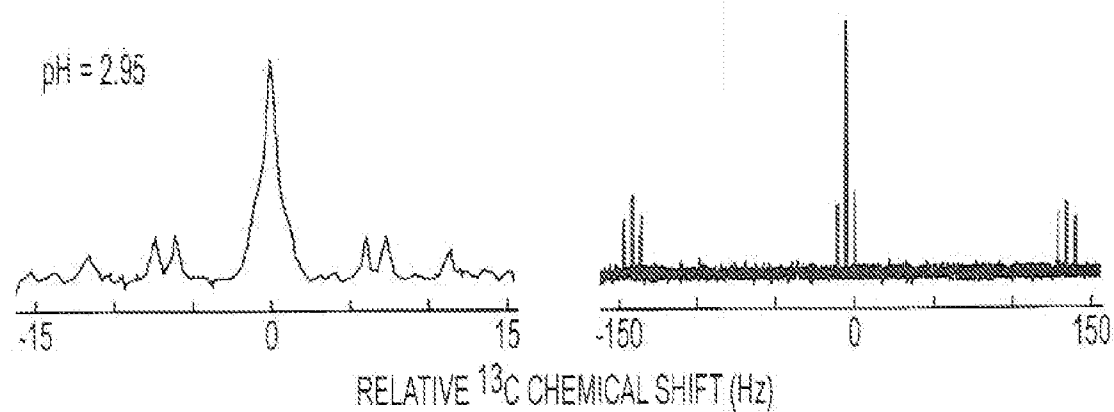
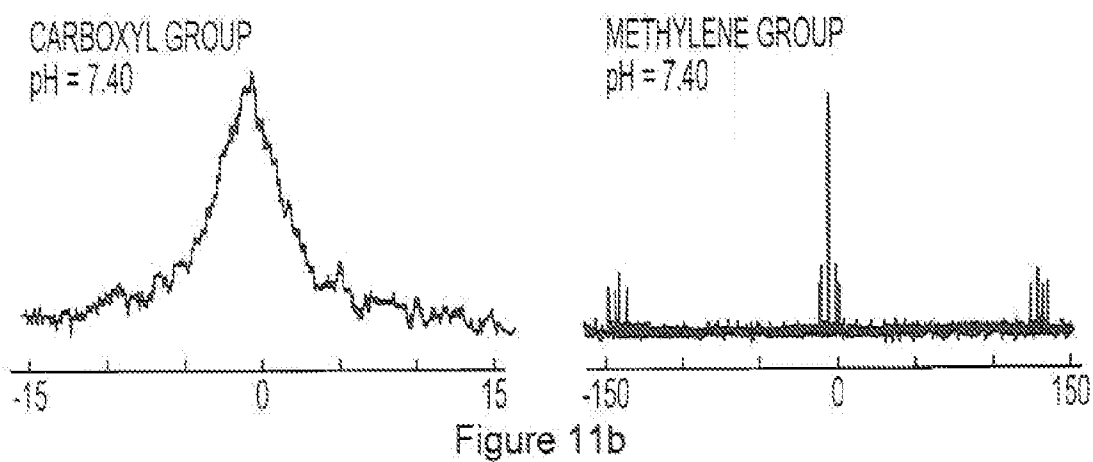


Figure 11c

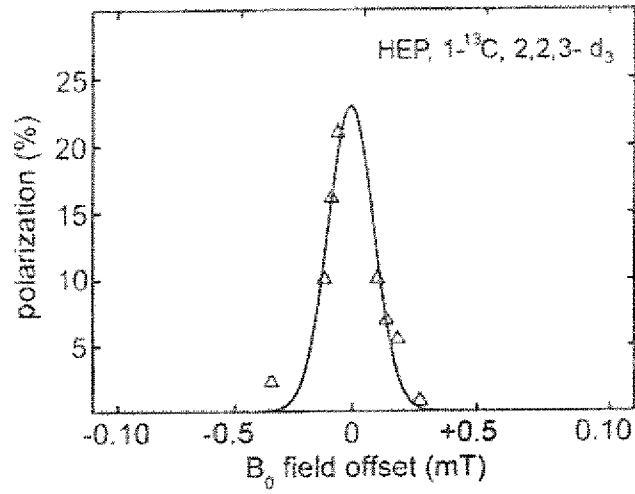


Figure 12

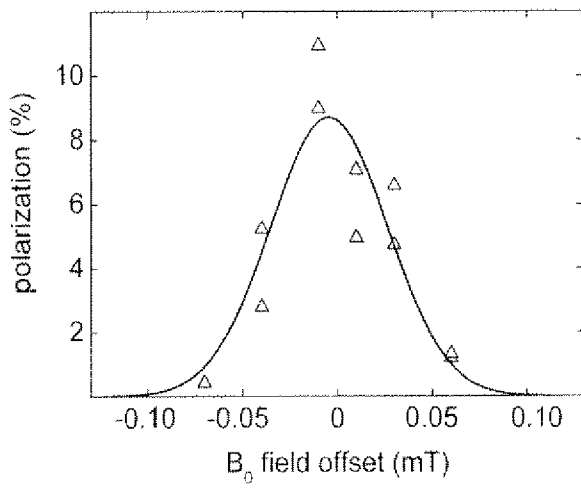


Figure 13a

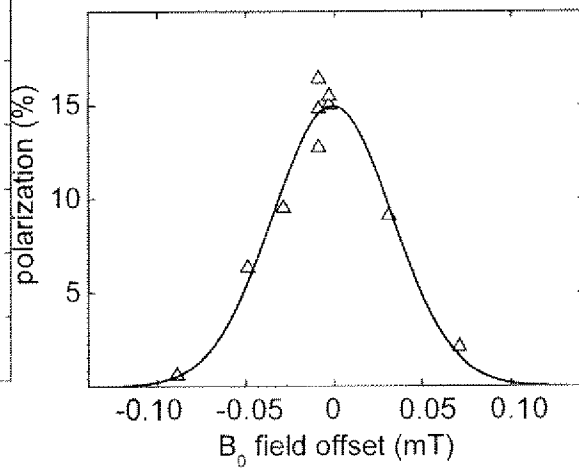


Figure 13b

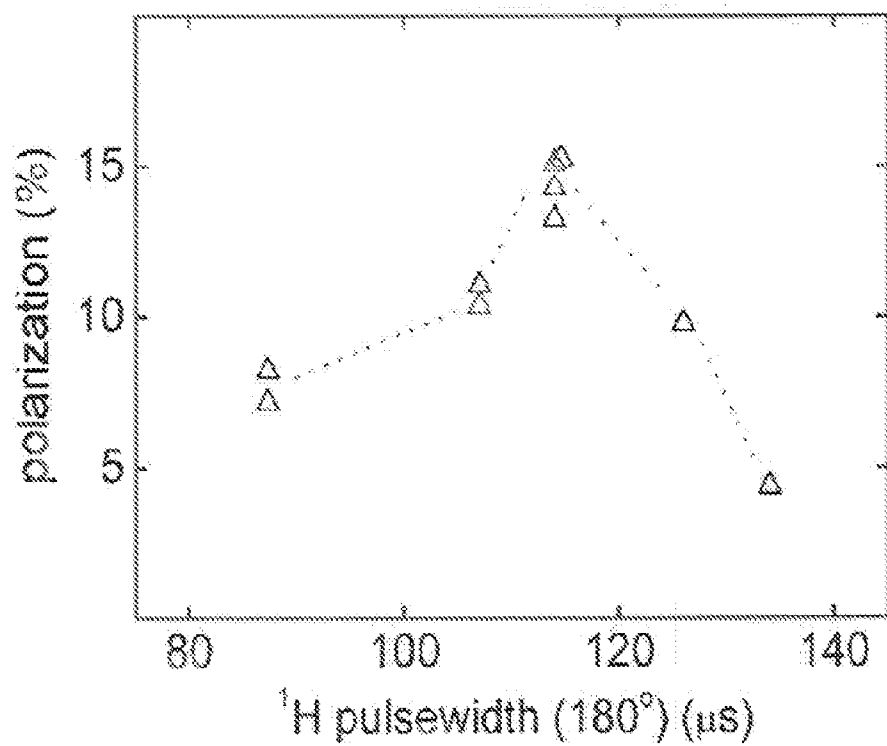


Figure 14a

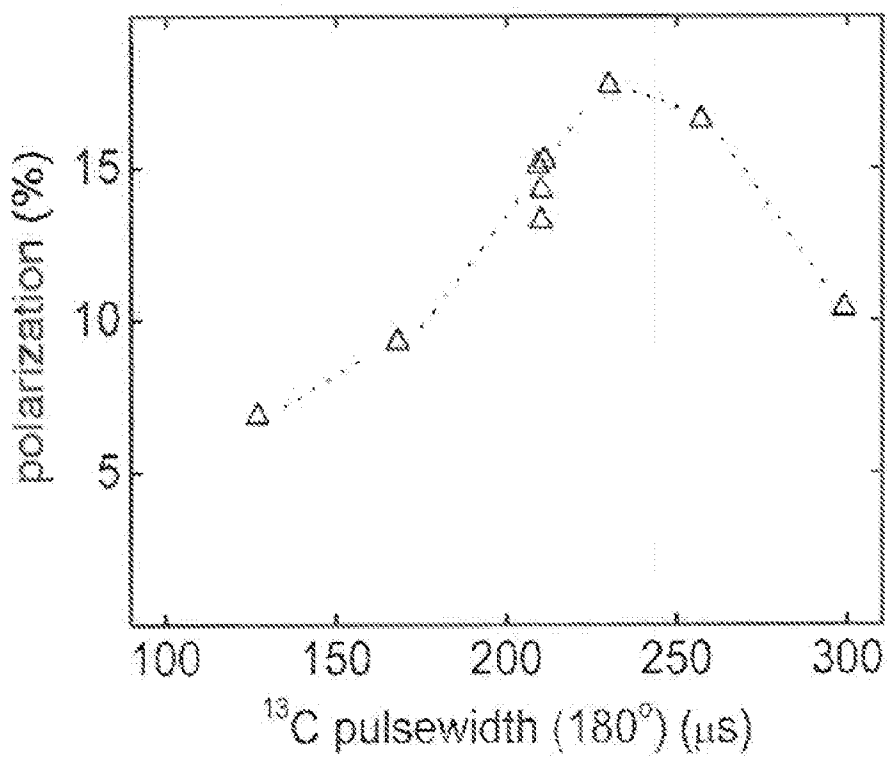


Figure 14b

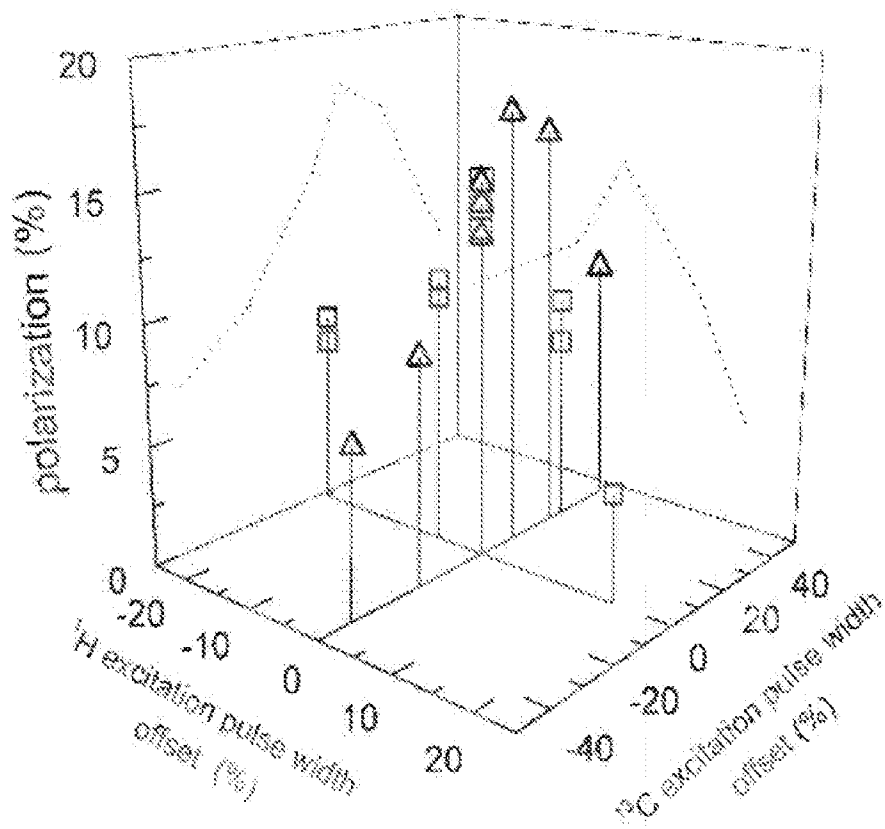


Figure 14c

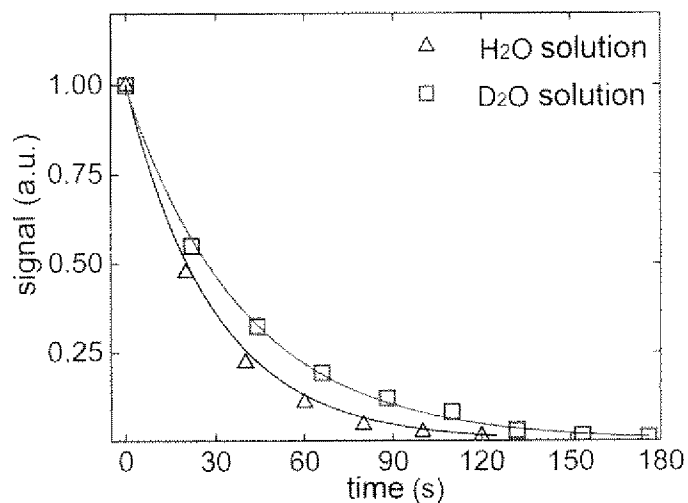


Figure 15

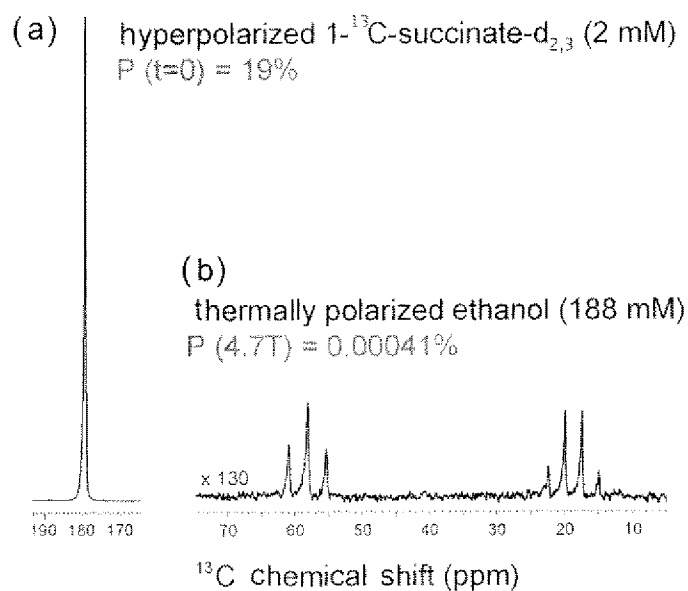


Figure 16

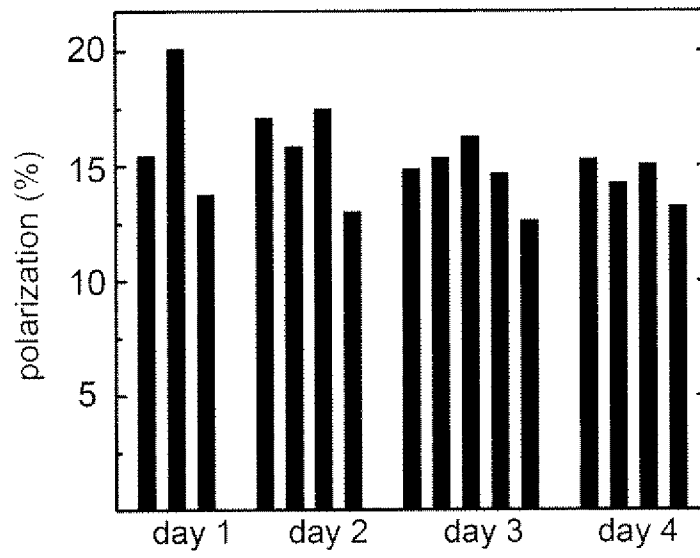


Figure 17

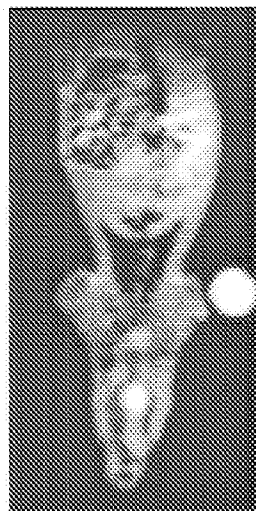


Figure 18

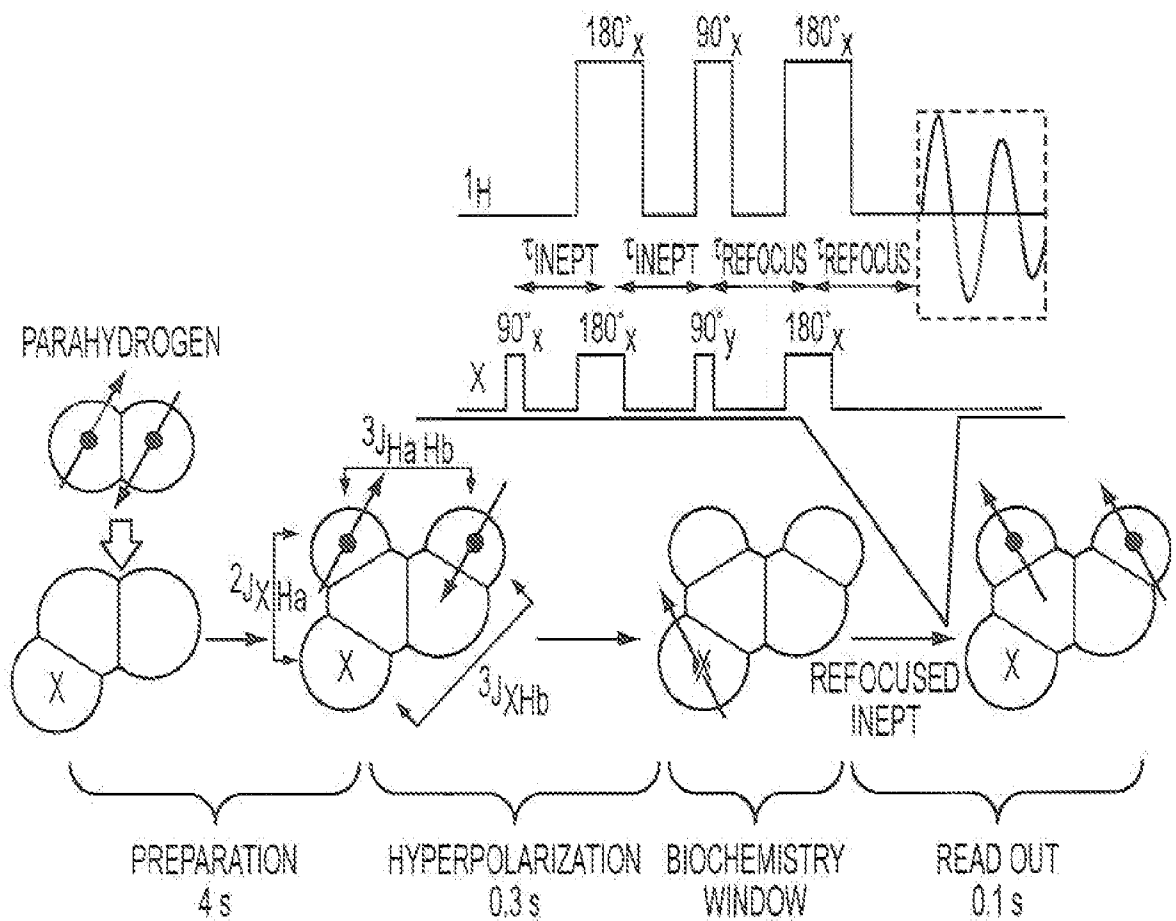


Figure 19

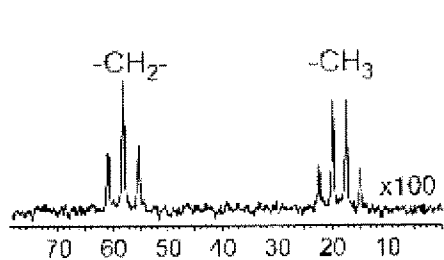


Figure 20a

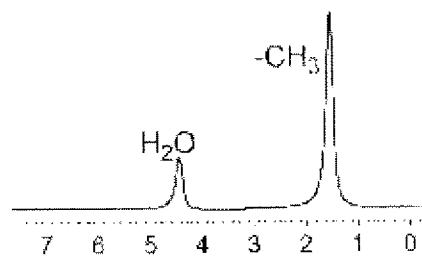


Figure 20b

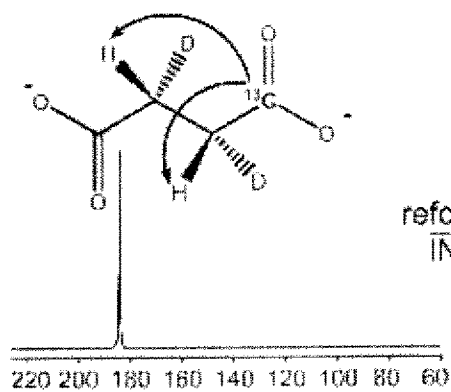


Figure 20c

refocused
INEPT

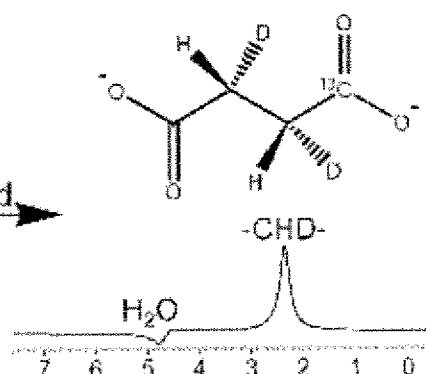


Figure 20d

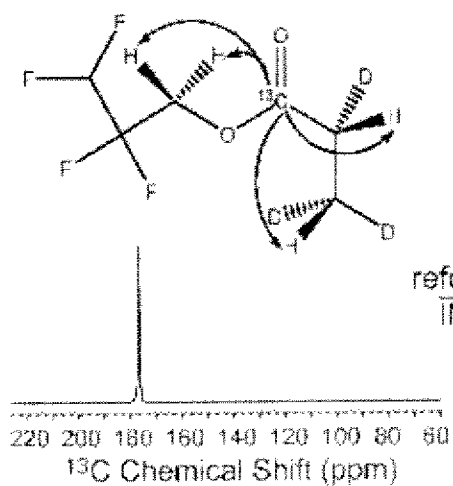


Figure 20e

refocused
INEPT

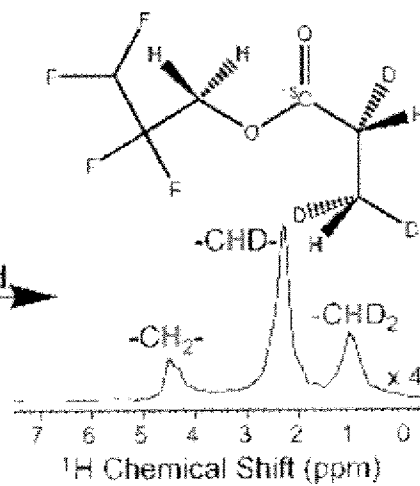


Figure 20f

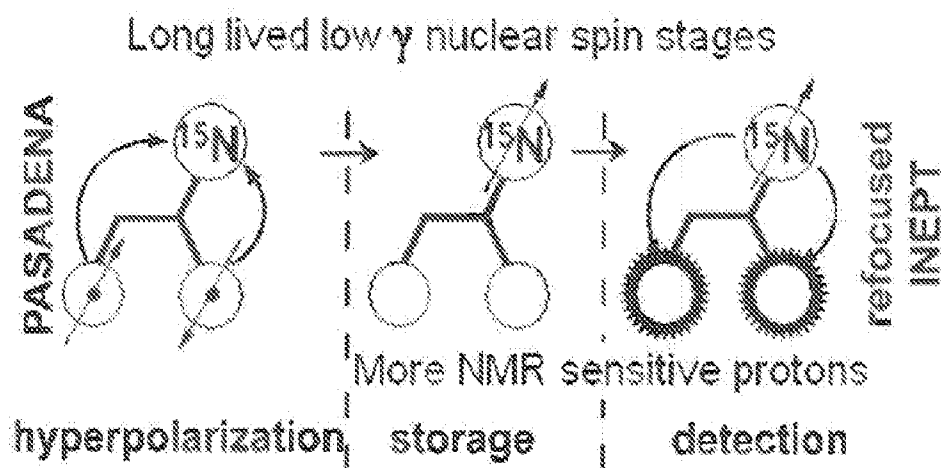


Figure 21

INTERNATIONAL SEARCH REPORT

International application No.
PCT/US2009/040568

A. CLASSIFICATION OF SUBJECT MATTER
 IPC(8) - A61B 5/05 (2009.01)
 USPC - 600/420
 According to International Patent Classification (IPC) or to both national classification and IPC

B. FIELDS SEARCHED
 Minimum documentation searched (classification system followed by classification symbols)
 IPC(8) - A61B 5/05, 5/055; G01V3/00 (2009.01)
 USPC - 324/307, 309; 424/9.3; 600/420;

Documentation searched other than minimum documentation to the extent that such documents are included in the fields searched

Electronic data base consulted during the international search (name of data base and, where practicable, search terms used)
 PatBase, Google Search

C. DOCUMENTS CONSIDERED TO BE RELEVANT

Category*	Citation of document, with indication, where appropriate, of the relevant passages	Relevant to claim No.
X	US 2006/0104906 A1 (ARDENKJAER-LARSEN et al) 18 May 2006 (18.05.2006) entire document	1-7, 9, 11-15, 17-24, 26, 28
--		-----
Y		8, 10, 16, 25, 27
Y	US 2006/0127313 A1 (GOLDMAN et al) 15 June 2006 (15.06.2006) entire document	8, 10, 16, 25, 27
A	US 6,727,697 B2 (FIAT) 27 April 2004 (27.04.2004) entire document	1-28

Further documents are listed in the continuation of Box C.

* Special categories of cited documents:

"A" document defining the general state of the art which is not considered to be of particular relevance	"T" later document published after the international filing date or priority date and not in conflict with the application but cited to understand the principle or theory underlying the invention
"E" earlier application or patent but published on or after the international filing date	"X" document of particular relevance; the claimed invention cannot be considered novel or cannot be considered to involve an inventive step when the document is taken alone
"L" document which may throw doubts on priority claim(s) or which is cited to establish the publication date of another citation or other special reason (as specified)	"Y" document of particular relevance; the claimed invention cannot be considered to involve an inventive step when the document is combined with one or more other such documents, such combination being obvious to a person skilled in the art
"O" document referring to an oral disclosure, use, exhibition or other means	"&" document member of the same patent family
"P" document published prior to the international filing date but later than the priority date claimed	

Date of the actual completion of the international search 29 May 2009	Date of mailing of the international search report 09 JUN 2009
Name and mailing address of the ISA/US Mail Stop PCT, Attn: ISA/US, Commissioner for Patents P.O. Box 1450, Alexandria, Virginia 22313-1450 Facsimile No. 571-273-3201	Authorized officer: Blaine R. Copenheaver PCT Helpdesk: 571-272-4300 PCT OSP: 571-272-7774